AD-A235 417

ATION PAGE

1. AGENCY USE ONLY (Leave blank)	2. REPORT DATE	3. REPORT TYPE AND DATES COVERED
	29 April 91	Final Report 1 Sep 90 - 28 Feb 91

4. TITLE AND SUBTITLE	5. FUNDING NUMBERS
The development of an improved convective initiation scheme for mesoscale numerical weather prediction models	65502F 3005/A1

6. AUTHOR(S)

Kenneth T. Waight III and Pamela E. Price

7. PERFORMING ORGANIZATION NAME(S) AND ADDRESS(ES)	8. PERFORMING ORGANIZATION REPORT NUMBER
Mesoscale Environmental Simulations & Operations, Inc. 185 Jordan Road Troy, NY 12180	28-3

AFOSR-TR 91 0493

9. SPONSORING/MONITORING AGENCY NAME(S) AND ADDRESS(ES)	10. SPONSORING/MONITORING AGENCY REPORT NUMBER
AFOSR/NC Building 410 Bolling AFB, DC 20332-6448	F49620-90-C-0057

DTIC
ELECTE
MAY 07 1991
S D
C

11. SUPPLEMENTARY NOTES

12a. DISTRIBUTION/AVAILABILITY STATEMENT	12b. DISTRIBUTION CODE
Approved for Public Release; Distribution is Unlimited.	

13. ABSTRACT (Maximum 200 words)

A three-dimensional nonhydrostatic cloud model, the Terminal Area Simulation System (TASS), is used to investigate the convective initiation process for an idealized case over central Florida where the forcing is provided by differential surface heating. The surface heating pattern is generated from high resolution land use data by making simple assumptions relating surface characteristics to particular land use types. The cloud model simulation produces a complicated field of both shallow and precipitating cumulus clouds. Current mesoscale parameterization schemes are evaluated for their ability to predict convective initiation. Analysis of the results shows that in the first half of the run, localized differential surface sensible heating produces small areas of deep convection associated with surface features. In the latter half of the simulation, mesoscale convergence develops due to the lateral boundary conditions and provides a mesoscale organization which is well resolved by a conventional measure of mesoscale moisture convergence. Subgrid scale convergence is very well correlated with convective activity. Results suggest that the cloud model is a valuable tool for the investigation of realistic convective initiation and evolution, and that a combination of mesoscale and subgrid scale properties are necessary for successful mesoscale modeling of cumulus convection.

14. SUBJECT TERMS		15. NUMBER OF PAGES
Convection, Mesoscale, Modeling, Cumulus, Initiation, Parameterization, Forecasting, Precipitation		51
		16. PRICE CODE

17. SECURITY CLASSIFICATION OF REPORT	18. SECURITY CLASSIFICATION OF THIS PAGE	19. SECURITY CLASSIFICATION OF ABSTRACT	20. LIMITATION OF ABSTRACT
UNCLASSIFIED	UNCLASSIFIED	UNCLASSIFIED	

91 5 07 023

PHASE I
FINAL PROJECT REPORT

SMALL BUSINESS INNOVATION RESEARCH
CONTRACT F49620-90-C-0057

THE DEVELOPMENT OF AN IMPROVED CONVECTIVE INITIATION SCHEME FOR MESOSCALE NUMERICAL WEATHER PREDICTION MODELS

PREPARED FOR :

Lt. Col. James Stobie
AFOSR/NC
Directorate of Chemical and Atmospheric Sciences
Building 410
Bolling AFB, DC 20332-6448

PREPARED BY :

MESO, Inc.
185 Jordan Road
Troy, NY 12180

April 29, 1991

91 5 07 023

The Development Of An Improved Convective Initiation Scheme For Mesoscale Numerical Weather Prediction Models

KENNETH T. WAIGHT III AND PAMELA E. PRICE

Mesoscale Environmental Simulations and Operations,Inc., 185 Jordan RD, Troy, NY 12180

ABSTRACT

A three-dimensional nonhydrostatic cloud model, the Terminal Area Simulation System (TASS), is used to investigate the convective initiation process for an idealized case over central Florida where the forcing is provided by differential surface heating. The surface heating pattern is generated from high resolution land use data by making simple assumptions relating surface characteristics to particular land use types. The cloud model simulation produces a complicated field of both shallow and precipitating cumulus clouds. Current mesoscale parameterization schemes are evaluated for their ability to predict convective initiation. Analysis of the results shows that in the first half of the run, localized differential surface sensible heating produces small areas of deep convection associated with surface features. In the latter half of the simulation, mesoscale convergence develops due to the lateral boundary conditions and provides a mesoscale organization which is well resolved by a conventional measure of mesoscale moisture convergence. Subgrid scale convergence is very well correlated with convective activity. Results suggest that the cloud model is a valuable tool for the investigation of realistic convective initiation and evolution, and that a combination of mesoscale and subgrid scale properties are necessary for successful mesoscale modeling of cumulus convection.

1. Statement Of The Problem / Identification And Significance Of The Innovation

Operational numerical models typically have difficulty forecasting precipitation during the warm season when large scale forcing is weak and most of the precipitation is convective in nature. A significant part of this forecast problem is caused by an inadequate physical understanding of cumulus convection on scales larger than that of an individual convective cell. For current operational and research mesoscale models, much of the physics of convection cannot be explicitly resolved on the model grid. As a

result, several sophisticated convective parameterization schemes have been proposed, which intend to represent these subgrid scale convective processes. An alternative to this implicit approach is to decrease the model grid size as much as possible and attempt to explicitly resolve the convection. Nonhydrostatic cloud models with very fine resolution (grid spacing less than 1 km) have been successful in directly simulating idealized convective clouds of various types. However, Zhang et al. (1988) demonstrated that for a meso-β-scale hydrostatic model, an implicit approach was necessary for the successful simulation of a summer mesoscale convective complex (MCC), even with a grid size of 12.5 km (near the lower limit for hydrostatic models). Therefore, until computer capabilities expand enough to allow nonhydrostatic cloud models to routinely cover meso-β domains, or until numerical methods are perfected which will allow the use of non-uniform grid meshes (e.g. "dynamically-adaptive" grids), convective parameterization schemes will continue to be necessary.

The problem of cumulus parameterization may be separated into two main components. First, convection must be *initiated* in the model at the proper place and time. Second, once initiation occurs, the model must successfully parameterize the subsequent *evolution* of the convection in time and space. Although available schemes differ in their treatment of both aspects, much more effort has been spent in evaluating and improving the evolution of convection. For example, evaluation of various schemes has often centered on the features of parameterized vertical profiles of convective heating and moistening (e.g. Kuo and Anthes, 1984), i.e. the evolution rather than the initiation. The relative importance of the two components depends mostly on one's immediate goal in running a simulation. If the purpose is to study a particular convective event or type of event in order to better understand its structure and evolution (research mode), then a poorly simulated distribution of convection outside of the area of interest is of relatively little concern. If on the other hand, the purpose is to successfully predict the location and timing of convection in real time (operational mode), then the ability of the scheme to initiate convection correctly becomes a necessity. Since meso-β-scale models currently exist only in the research environment and have mostly been used for case studies where the focus is on one particular feature or storm,

very little has been done to verify the ability of current schemes to predict the spatial and temporal *distribution* of convection.

A substantial portion of the initiation problem is caused by inadequate knowledge of the characteristics of the earth's surface (soil moisture, surface albedo, vegetation, etc.) and of the three-dimensional structure of the atmosphere. Mesoscale models can not possibly forecast the evolution of convection correctly if the upper air data used in the model initialization misses important features such as convergence or moisture gradients. Even given "perfect" model initial conditions however, currently available cumulus parameterization schemes would predict significantly different distributions of convection due to their very different criteria for convective initiation. Fritsch and Chappell (1980) presented a scheme intended for meso β-scale models which has shown considerable skill in simulating midlatitude warm season convective systems (Zhang and Fritsch, 1986; Zhang and Fritsch, 1988; Zhang et. al, 1989). Convection begins in this scheme at a grid point if a parcel lifted to its lifting condensation level (LCL) is positively buoyant (i.e. if there is available buoyant energy), and if a one-dimensional cloud model is subsequently able to form a cloud of sufficient depth above the LCL. In addition, the mesoscale (grid-resolvable) vertical velocity at the LCL exerts a strong role through a special temperature perturbation term which is added to the temperature of the lifted parcel. Frank and Cohen (1987) have formulated a meso-β-scale scheme which defines threshold amounts of both low-level mass convergence and latent instability as being necessary conditions for the occurrence of convection. Anthes (1977) presents a scheme following Kuo (1965) which also requires grid scale convergence. The difference in the two types of closure assumptions is subtle but important. For the Fritsch-Chappell scheme, mesoscale vertical velocity is a contributing factor but not a necessary condition. Convection could occur without any dynamic forcing for a sufficiently unstable sounding. The Frank-Cohen scheme (originally intended for tropical application) and the Kuo-type schemes *require* the presence of mesoscale convergence. In each case, the two controlling factors are thermodynamic instability and mesoscale dynamic forcing (mass convergence or hydrostatic vertical velocity). However, the relative importance of these two factors for different types of initiation mechanisms is not at all clear.

Cooper *et al.* (1982) studied sea breeze convection over South

Florida found that convergence on two scales were involved in convective initiation. First, a peninsular scale convergence is related to the sea breeze circulation which occurs with regularity. This convergence triggered thunderstorms beginning in the late morning. Second, outflows from the original convection generated convergence on smaller scales and often initiated new convection.

It is also possible that other parameters could be useful such as some measure of the subgrid scale inhomogeneity of surface characteristics or an indicator of the state of the planetary boundary layer to represent the vigor and variability of rising thermals. Chen and Orville (1980) found that mesoscale convergence weakened an inhibiting temperature inversion and moistened the lower atmosphere in a two-dimensional cloud model simulation, leading to stronger thermals and deeper convection. Balaji and Clark (1988) and Redelsperger and Clark (1990) have investigated the interactions between boundary layer instabilities and the formation of deep convection.

In addition, the dependence of any initiation criterion on model grid size is very poorly understood. It is believed that a significant improvement in the definition of criteria for the initiation of deep convection by a cumulus parameterization scheme would result in a substantial improvement in the ability of a mesoscale model to correctly simulate the timing and location of warm season precipitation.

This research has focused on the initiation process rather than the evolution of the thunderstorms, in an attempt to investigate what is believed to be the least understood area of the overall convective problem. A fundamental difficulty in studying initiation is that scales of motion from the size of an individual updraft (100 m) to a large scale atmospheric wave (1000 km) interact in a complex way to form thunderstorms of various sizes. The innovative aspects of this research fall in two separate areas, the use of a cloud model to study the initiation problem, and the high resolution surface flux treatment used to initiate the convection.

Nonhydrostatic cloud models have traditionally been used to investigate the characteristics of one particular convective system, be it a supercell storm, multicellular convection, etc. Because most of these simulations were done in the research mode to better understand the dynamics and/or microphysics of a particular storm, verification against observations was done assuming that the modelled storm developed at the

same time as the observed one. Then the structure and evolution of the two storms may be compared and studied. There have been several different approaches for initiating the convection, from thermal perturbations (the most common) to heating or cooling functions and mesoscale forcing functions. Generally, the method chosen is balanced between the desire for a reasonable simulation and the current computational restrictions. The methods mentioned above are examples of forcing which minimize the "start-up" time before the convections forms so that the resources can be effectively used to study the storm itself.

This approach works well until the initiation becomes the area of interest. At this point, a new approach toward initiation is required which allows the simulation of the pre-convective environment and the transition from shallow to deep convection as well. As computers continue to become faster and less expensive, these types of simulations are now becoming possible. As a first step, convection was initiated through forcing by small scale (750 m) variations in surface sensible and latent heating to demonstrate the feasibility of the approach.

The original intention was to use idealized surface heating patterns to force convective circulations, but the availability of very high resolution (200-400 m) Florida land use data in connection with another project made it possible to use a much more complex and realistic pattern. The complex patterns of cloudiness and precipitation produced by the resulting TASS simulations were more complicated than traditionally modeled clouds and were visually very impressive. In the proposed Phase II research, improvements to the cloud model initial and boundary conditions will permit an actual comparison of cloud model results to observations on specific days. Although such a rigorous verification has not yet been done, the Phase I results were extremely encouraging. The results suggest that cloud model physics can sufficiently model real clouds given real initial conditions. Since a significant portion of the ordinary convection occurring daily in the warm season over much of the U.S. is believed to be forced by the type of surface variability modeled in this research, the potential exists for substantial improvement in thunderstorm prediction.

2. Experimental Design

The Phase I proposal stated that a successful result of this research would be determined by success in two areas, one technical and one scientific. First, the cloud model must be shown to be technically capable of simulating several realistic and clearly-defined convective initiation events from a complex distribution of sensible heating alone. Second, analysis of the cloud model results should suggest, for the case of differential surface heating, that a clear and physically defensible relationship exists between one or more parameters and convective occurrence on the meso-β-scale. Furthermore, the relationship should be able to quantitatively diagnose convection more accurately than existing schemes.

2.1 The TASS Model

The three-dimensional Terminal Area Simulation System (TASS) cloud model is nonhydrostatic and compressible with prognostic equations for momentum, potential temperature, pressure and six bulk water categories: water vapor, cloud droplets, ice crystals, rain, snow and graupel/hail. It includes a complex microphysical parameterization scheme following Lin et al. (1983) and Rutledge and Hobbs (1983). For further details on the model formulation, see Proctor (1987a). Verification tests of the model have been completed for several different types of convection, from weak multicellular Florida convection to long-lasting supercell hailstorms with successful results (Proctor, 1987b). In addition, the model has recently been applied to the simulation of mountain-forced wave evolution using initialization from a high-resolution MASS mesoscale simulation.

2.2 TASS Initial Conditions

The sounding used to initialize the TASS model was the 0000 GMT Tampa sounding from June 22, 1982 (see Fig. 1). This is a typical sounding for Florida with moderate instability (a lifted index of -4), and light winds from 3 to 15 m s^{-1} which veer from southwesterly at the surface to northwest aloft. The profile is fairly moist other than a dry layer at 450

mb and above 250 mb. There were widespread areas of convection over the Florida peninsula during this day which weakened after sunset.

2.2.1 Surface heat and moisture fluxes

The most significant departure in this application of the cloud model from previous uses is the forcing used to produce convection. In most of the previous applications, the goals involved studying the evolution of convection once formed, and generally the location of the initial forcing and the resulting convection is chosen to be in the center of the domain so that boundary effects are minimized and the convection can be kept within the domain. In previous sensitivity tests, the evolution of the deep convection once formed has not been found to be overly sensitive to the initial perturbation used although stronger forcing can increase the overall intensity of the convection and forcing which is too weak will not produce any convection.

However, in order to study the timing and location of convective initiation, the conditions which produce the convection become the area of interest. As a first step, a complicated, realistic pattern of surface heating and moistening was used, along with a single sounding to define the environmental profiles of temperature, dew point and winds. This means that there are no initial horizontal variations such as dry lines, old convective boundaries or areas of convergence, features which are known to produce regions of preferred convection. Even in this simplified environment, the convection develops in certain areas of the grid and not others, which allows the investigation of relationships on different scales between environmental parameters and convection.

Land use data covering the state of Florida was obtained from the U.S. Geological Survey. The resolution of the gridded data is 200 m in urban areas and 400 m otherwise. Each grid box is classified as one category, represented by a two digit number. The first digit indicates the "Level I" category (major land use types), the second indicates the Level II subcategory (finer distinctions). Table 1 lists the complete set of land use categories. Fig. 2 is a color image of land use data covering most of Central Florida, representing each land use category as a different color.

As a first attempt at generating realistic patterns of surface heating and moistening from high resolution surface data, two parameters were

assigned to each Level I category, surface albedo and Bowen ratio, the ratio of the sensible to latent heat flux. Then an assumed value of net radiation was partitioned into sensible and latent heat fluxes based on these values. The surface characteristics and resulting fluxes are shown in Table 1. The spatial pattern of the sensible and latent heat fluxes over the cloud model domain is shown in Fig. 3. The peak sensible (latent) heating rate was approximately 200 W m^{-2} (450 W m^{-2}), and the area in the northeast corner is over water.

Once the heating and moistening rates were generated for each surface point in the TASS model, they were input into TASS and integrated each timestep at the first model level above the ground (150 m for this case). The heating and moistening rates were held constant with time unless a cloud formed above that point, at which time the rates were reduced by 75%. This is a crude estimate of the effect of cloudiness on surface heating under clouds. The lateral boundary conditions of the model for potential temperature and water vapor are determined from upstream time differencing if the flow normal to the boundary is outward and relaxed to the initial environmental values if the flow is directed inward. Therefore, since no information on surface fluxes is available outside the domain, this results in unmodified (unheated and unmoistened) air being advected into the domain on inflow boundaries. The impact of this effect is proportional to the low-level wind speed which is light for the sounding chosen. In sensitivity tests, low-level winds of 3-5 m/s resulted in convection which developed further north (downstream) and was advected out of the domain by the end of the simulation. The model has the ability to translate with convection or at a specified constant speed but with fixed surface conditions (sensible and latent fluxes), this would not be physically realistic. In Phase II, this problem will be studied and resolved, possibly with a movable domain capable of ingesting new surface information as it translates.

2.3   Diagnostic and statistical approach

Full three-dimensional fields (u, v, and w-components of motion, temperature, mixing ratio and pressure) were saved at the full TASS resolution (750 m) every 15 minutes for an hour before the convection began and then through the rest of the simulation. These fields were then

averaged to coarser resolutions, chosen as exact multiples of 750 m. These averaged datasets, along with the full resolution fields, form the basis for the following analyses. The grid size used for most of the discussion in this study is 8.25 km. That size is large enough to represent the lower end of the meso-β-scale, yet small enough to resolve the mesoscale convergence, as well as provide enough mesoscale grid boxes for statistical interpretation.

A mesoscale area was considered to be convective if the accumulated precipitation at the ground was at least 0.1 mm when averaged over the grid box. After some initial analysis, it was found that instantaneous values of model variables and rainfall rates were very difficult to correlate because of the complicated time evolution of the simulation. Instead, 30 minute averages of all model fields, and rainfall accumulated over 30 minute time periods formed the basis for subsequent analysis.

A group of 17 parameters was chosen for analysis of the cloud model results. The parameters can be broken into four groups; they are shown in Table 2. Two basic statistical approaches were used. First, individual parameters were plotted against accumulated rainfall at various times. Second, various criteria for convective initiation were tested against actual rainfall by using two measures used in quantitative precipitation verification, THREAT and BIAS scores, defined as follows:

$$THREAT = \frac{CF}{O + (F - CF)},$$

(2.1)

$$BIAS = \frac{F}{O},$$

(2.2)

where:

O = observed (averaged from cloud model) number of grid points with convection,

F = forecast number of grid points with convection (specified by each particular set of criteria),

CF = number of correctly forecast grid points (points with convection both observed and forecast).

The THREAT score rewards correctly forecast grid points and also

imposes a penalty (F-CF in the denominator) for forecasting convection where none occurs. A THREAT score of one is perfect, while a score of zero indicates no correctly forecast grid points. The BIAS score distinguishes between overprediction and underprediction. The objective scores for each method were plotted as a function of time.
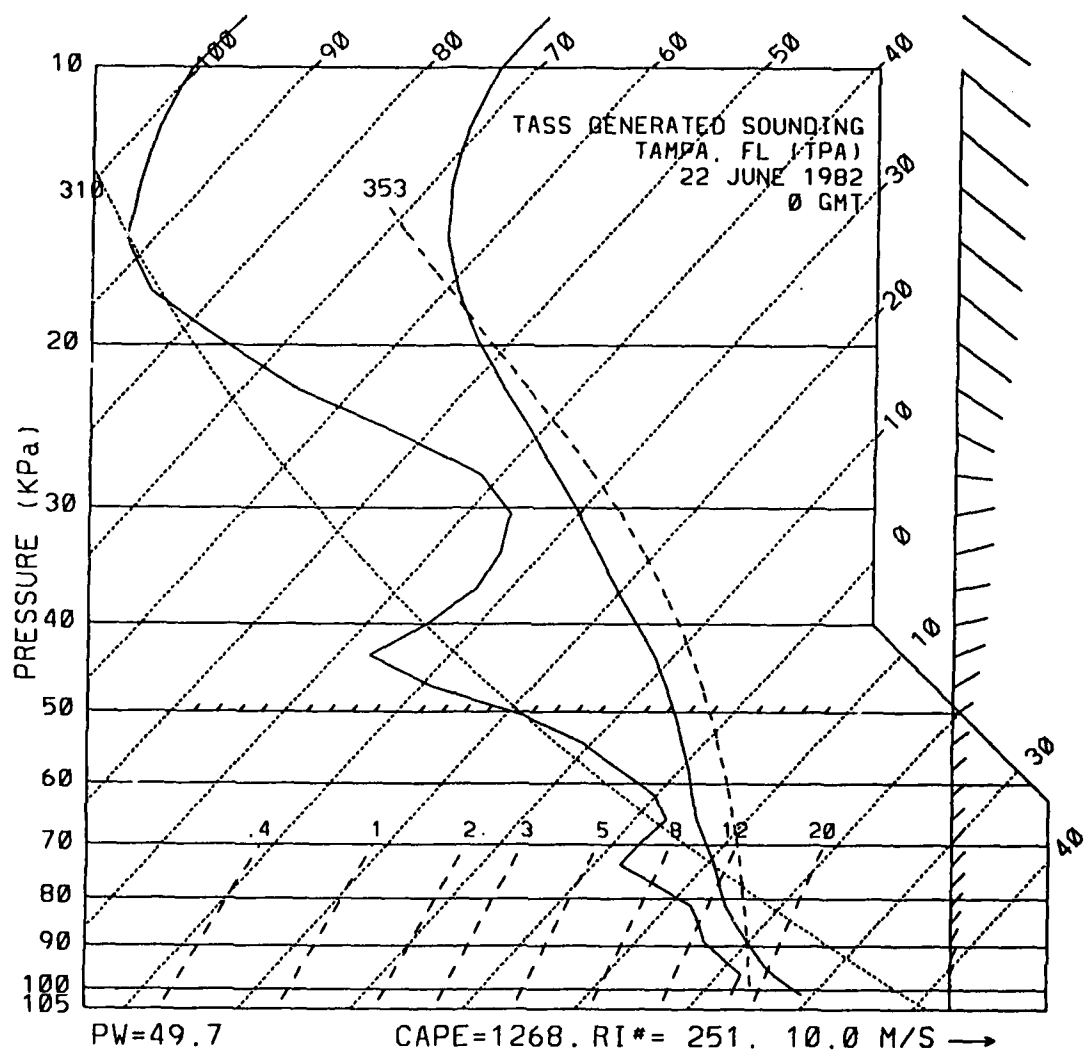
Figure 1 Skew-T diagram for Tampa, Florida on June 22, 1982 at 00 GMT.

Figure 2 (Following page) Color image of Florida land use data at 1 km resolution. Each color represents a major land use type. Red: urban, orange (and brown): agricultural land, yellow: rangeland, green: forested land, dark blue: bodies of water, light blue: wetland, gray (hard to see): barren land.

Land Use Category	Albedo	Bowen Ratio
11 Residential	.15	.80
12 Commercial and Services	.22	.90
13 Industrial	.20	.88
14 Transportation, Communications, Utilities	.20	.90
15 Industrial and Commercial Complexes	.20	.85
16 Mixed Urban or Built-up Land	.20	.85
17 Other Urban or Built-up Land	.20	.85
21 Cropland and Pasture	.20	.45
22 Orchards, Groves, Vineyards, Nurseries, etc.	.20	.45
23 Confined Feeding Operations	.20	.45
24 Other Agricultural Land	.20	.45
31 Herbaceous Rangeland	.15	.60
32 Shrub and Brush Rangeland	.15	.60
33 Mixed Rangeland	.15	.60
41 Deciduous Forest Land	.15	.30
42 Evergreen Forest Land	.15	.30
43 Mixed Forest Land	.15	.30
51 Streams and Canals	.10	.00
52 Lakes	.10	.00
53 Reservoirs	.10	.00
54 Bays and Estuaries	.10	.00
61 Forested Wetland	.10	.20
62 Nonforested Wetland	.10	.20
71 Dry Salt Flats	.30	.70
72 Beaches	.30	.70
73 Sandy Areas Other than Beaches	.30	.70
74 Bare Exposed Rock	.30	.70
75 Strip Mines, Quarries, Gravel Pits	.30	.70
76 Transitional Areas	.30	.70
77 Mixed Barren Land	.30	.70

Table 1 Land use classifications with estimated surface characteristics.
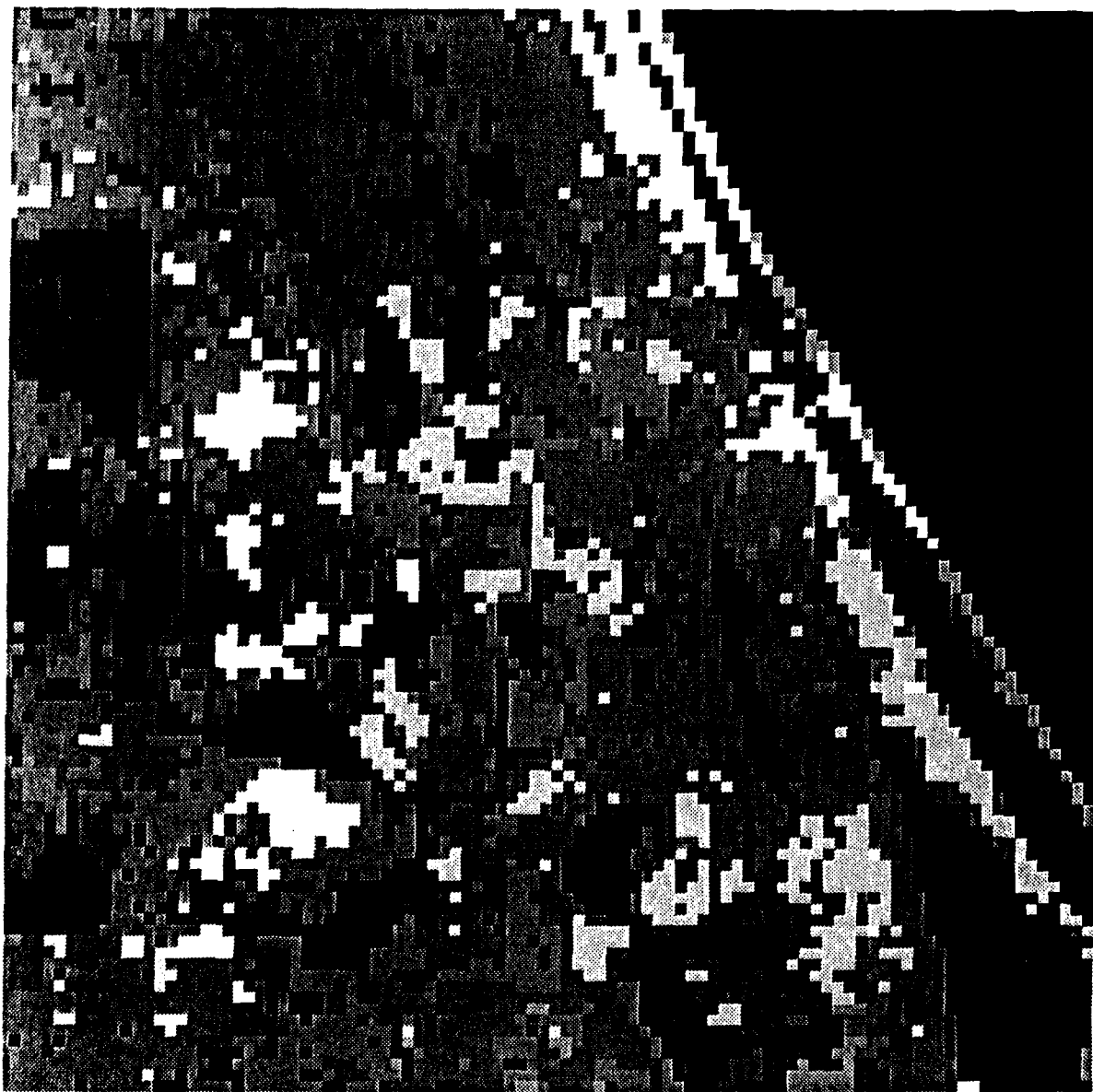
Figure 3a Pattern of sensible heat flux over the TASS model domain derived from land use data. Light areas represent large fluxes. The area covered extends from just north of Orlando, FL on the southwest corner to Daytona Beach, FL on the northeast coastline. The resolution of the image is 750 m.
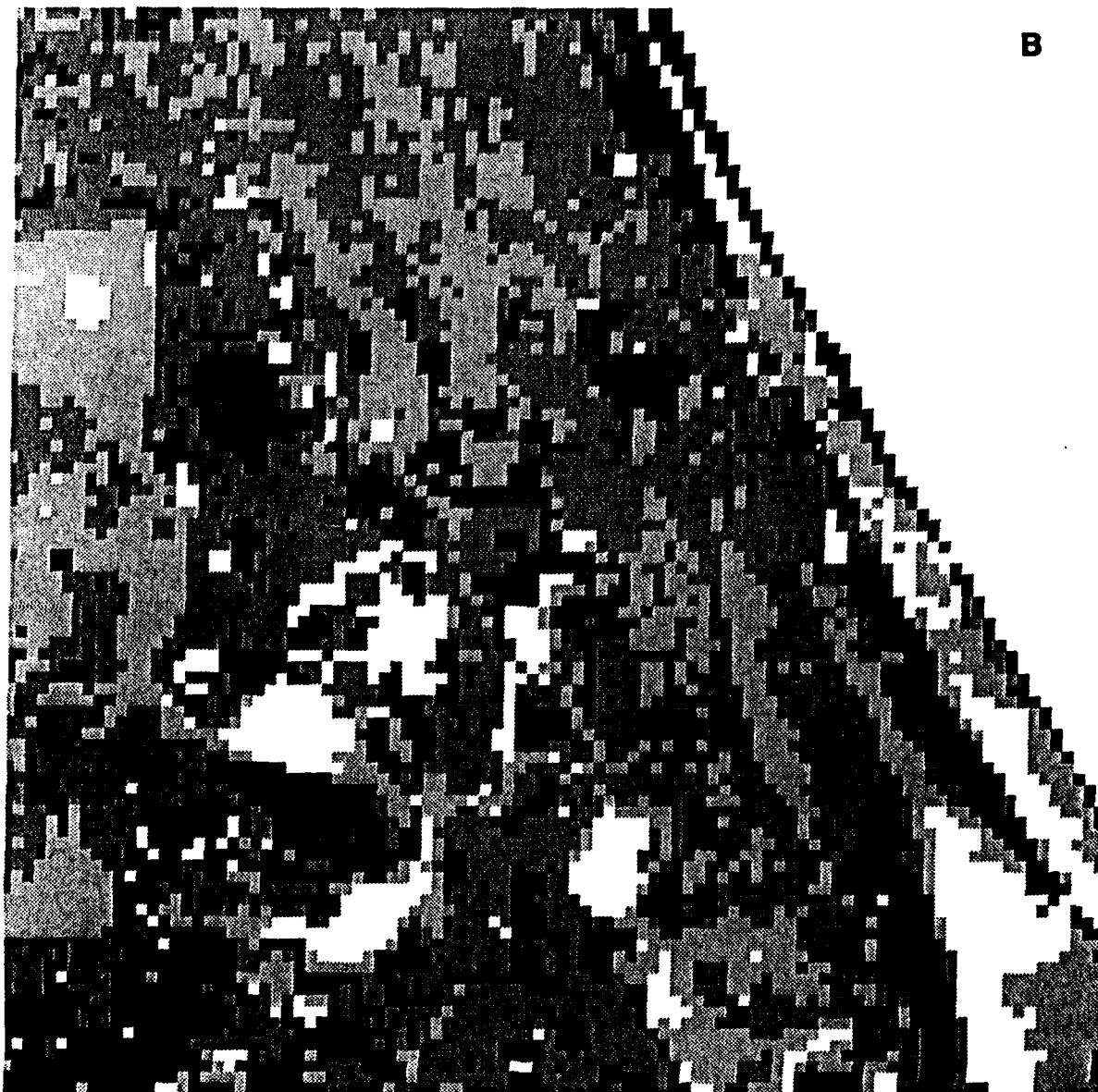
Figure 3b Same as Fig. 3a except for latent heat flux.

Stability Parameters	1. Convective Available Potential Enegy (CAPE)
	2. Negative Sounding Area
Convergence Parameters	3. Level 1 Convergence
	4. Max Convergence below 500 mb
	5. 700 mb Convergence
	6. Column Moisture Convergence
Vertical velocity Parameters	7. Max averaged w below 500 mb
	8. Averaged w at 700 mb
	9. Max diagnostic w below 500 mb
Subgrid Parameters	10. Max subgrid level 1 temperature
	11. Std. Dev. of subgrid level 1 temperature
	12. Max subgrid w below 500 mb
	13. Max subgrid CAPE
	14. Min subgrid negative area
	15. Max subgrid level 1 convergence
	16. Average sensible heat flux
	17. Std. Dev. of subgrid sensible heat flux

Table 2 List of convective parameters for statistical analysis.

3. Physical Analysis Of Model Results

The TASS cloud model was run for 180 minutes (three hours) of simulation time over a 98x98x33 domain with a horizontal resolution of 750 m and a stretched vertical mesh ranging from 300 m at the surface to 1 km at the top of the grid. The model domain was 73.5 km in the x- and y-directions and 18 km deep.

Fig. 4 shows the boundaries of the cloud field (cloud water, cloud ice, rain and snow) over the evolution of the convection from 60 to 180 min. A field of small cumuli began to form after 60 minutes of simulation time (Fig. 4a) and one of the cells in the northwest quadrant of the grid continued to deepen to 9 km. Rain began to fall and reached the ground after 90 minutes. The peak updraft strength of this first deep cell was 12-14 m s^{-1} and the peak reflectivity was 57 dBz. As the complicated pattern of surface heating and moistening continued, a second group of cells scattered throughout the domain continued to develop and reached depths of 11 km and peak updrafts of 16 m s^{-1}. These cells are visible in Fig. 4b at 90 minutes and several new areas of rainfall began reaching the ground between 90 and 120 minutes. As the time vs. height plots of peak vertical velocity (Fig. 5a) and peak reflectivity (Fig. 5b) show, each successive set of cells develops with stronger updrafts and higher cloud tops, the four cycles ending at approximately 90, 120, 150 minutes and the last after the 180 minute end of the simulation.

The increased development for the second cycle between 90 and 120 minutes does not appear to be redevelopment from previous cells since the new cells are well separated in space from earlier development. These cells still seem to be essentially forced by continued surface heating. However at later times (after 120 minutes) the convection became very strongly tied to the increasing convergence near the boundaries as well as the areas of previous convection and their subsequent outflows boundaries.

Fig. 6 shows the horizontal wind vector fields near the surface from 90 to 180 minutes. At 90 and 120 minutes, the coastline is visible in the northeast corner and the winds over the water have shifted to the southeast to form an area of convergence at the coastline. By 120 minutes, several weak outflows are visible and the effects of the increased

convergent flow in from the west and south boundaries is visible as the heating over the interior of the grid continues. The convergence is most pronounced along the south and west inflow boundaries due to the interaction between the low level heating and mean southwesterly flow. This simulation is representative of a generic island with unheated regions circumscribing the interior heated area. The southwest corner can be thought of as a convex land-water boundary with enhanced convergence. Over the length of the simulation, the "sea-breeze" circulation strengthens and advects inward from the boundaries as the strongest convection does also. Through 150 to 180 minutes, the strength of the convective outflows increase (with maximum speeds greater than 10 m s^{-1}) especially due to a strong cell in the southwest quadrant and the developing complex in the southeast quadrant. The area in the southeast quadrant of the domain became well-organized by the end of the simulation with a peak accumulated rainfall amount of almost 2 inches.

When comparing the structure between cells from 90 to 120 minutes with those after 150 minutes, the isolated nature of the earlier cells is noticeable. Fig. 7 shows vertical slices through the vertical velocity and radar reflectivity cores of the first cell to produce rain. Both the updraft and the reflectivity core are very cellular and isolated. Also, the updraft and the rainfall are colocated in the same column with little sloping to the updraft. By comparison, the velocity and reflectivity slices through the convective area in the southeast quadrant at 180 minutes (Fig. 8) shows a complex structure of interacting and merging cells which are forming somewhat along a line. The updrafts are actually sloping to the northeast with height so the slice shown only captures part of one updraft. The updraft is visible as two separate bubbles, the first one centered at a height of 10 km, and the second newer updraft centered at 5 km. This is similar to observations of Florida convection reported during the FACE experiment (Cunning and DeMaria, 1986; Cunning *et al.*, 1986) and modeled by Proctor (1987b). Overall, there is an increase in the width and strength of the updrafts over the length of this simulation as well as an increase in the areal coverage of the radar echoes. The increase in updraft width and strength as convergence in the domain increases is consistent with results from Chen and Orville (1980), who found that adding mesoscale convergence in two-dimensional simulations produced deeper broader clouds. Fig. 9 shows low-level horizontal radar reflectivity slices

at 105 and 180 minutes. The earlier echoes are smaller and isolated when compared to the complex later echo patterns. The reflectivity pattern at 180 minutes forms an oval ring-shaped pattern with a echo-free area in the center. This is most likely a result of the land-water boundary in combination with the inflow boundary conditions.
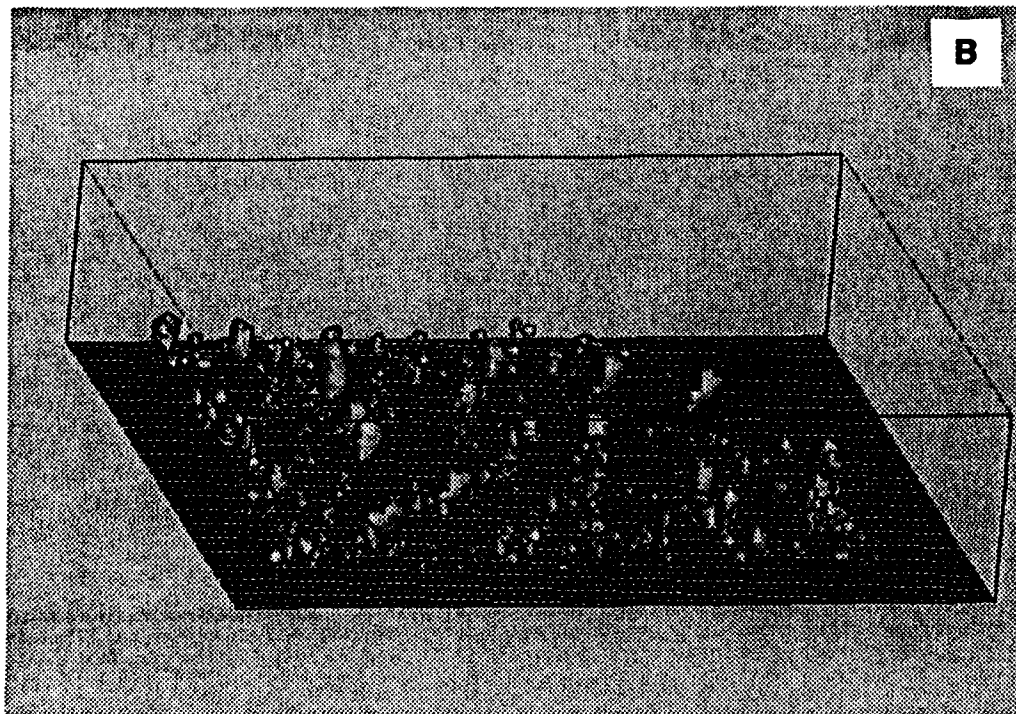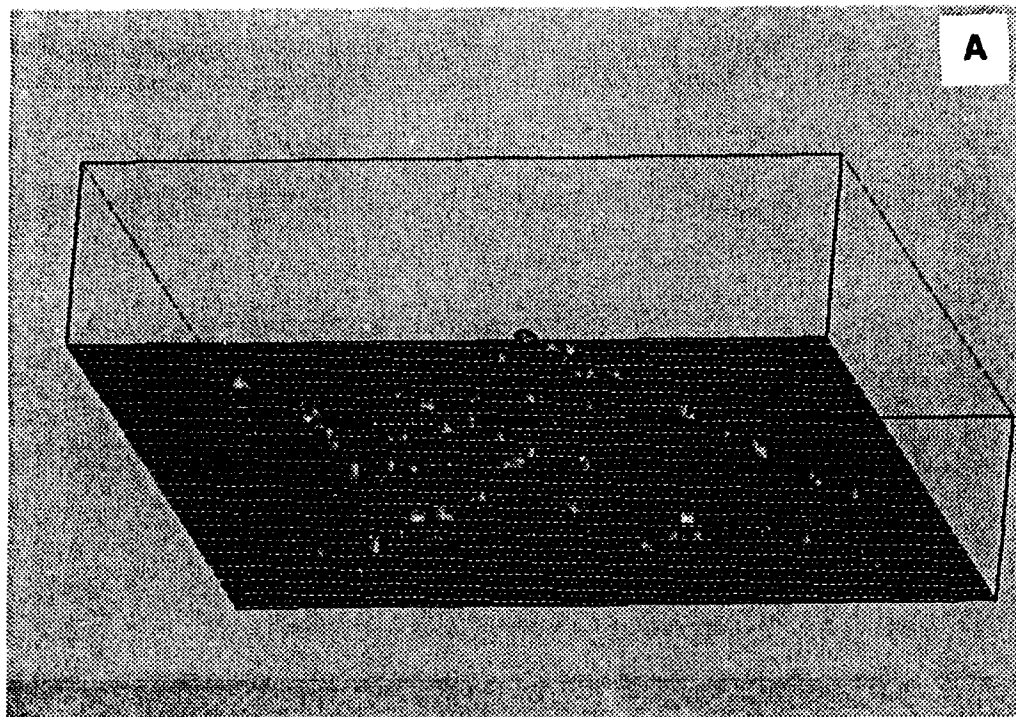
Figure 4 Three-dimensional perspective of the TASS cloud model output after (a) 60 min, (b) 90 min, (c) 120 min, (d) 150 min and (e) 180 min of simulation time. The light gray surfaces represent the cloud and rain fields and the cold air outflow is represented by the darker gray (turquoise in the color figure) near the surface. The view is from the south looking north.
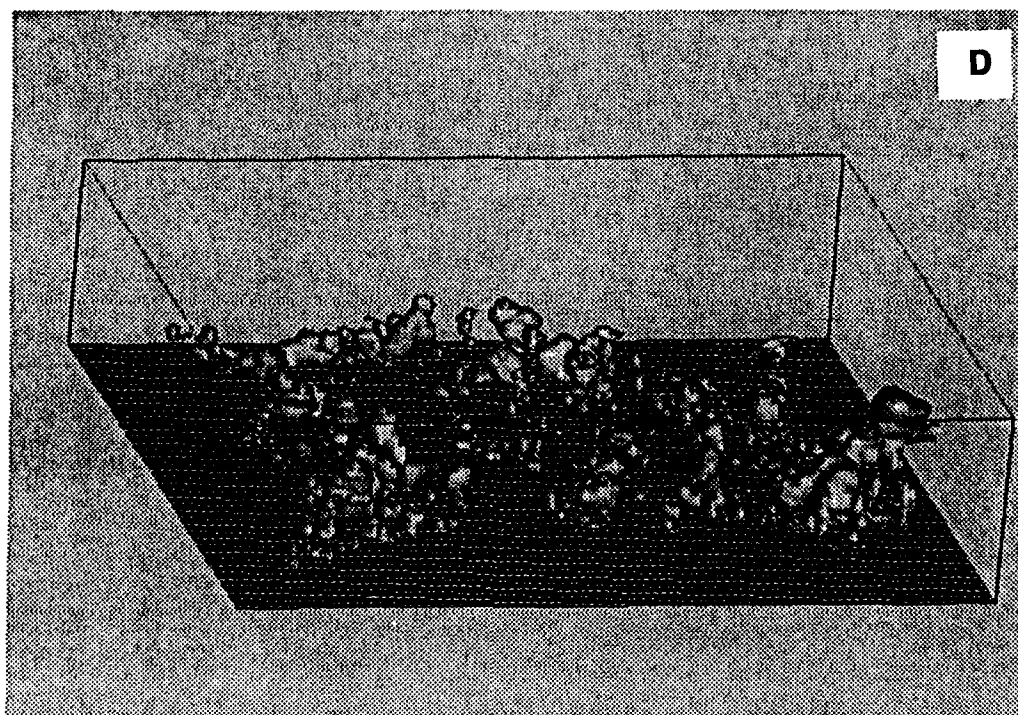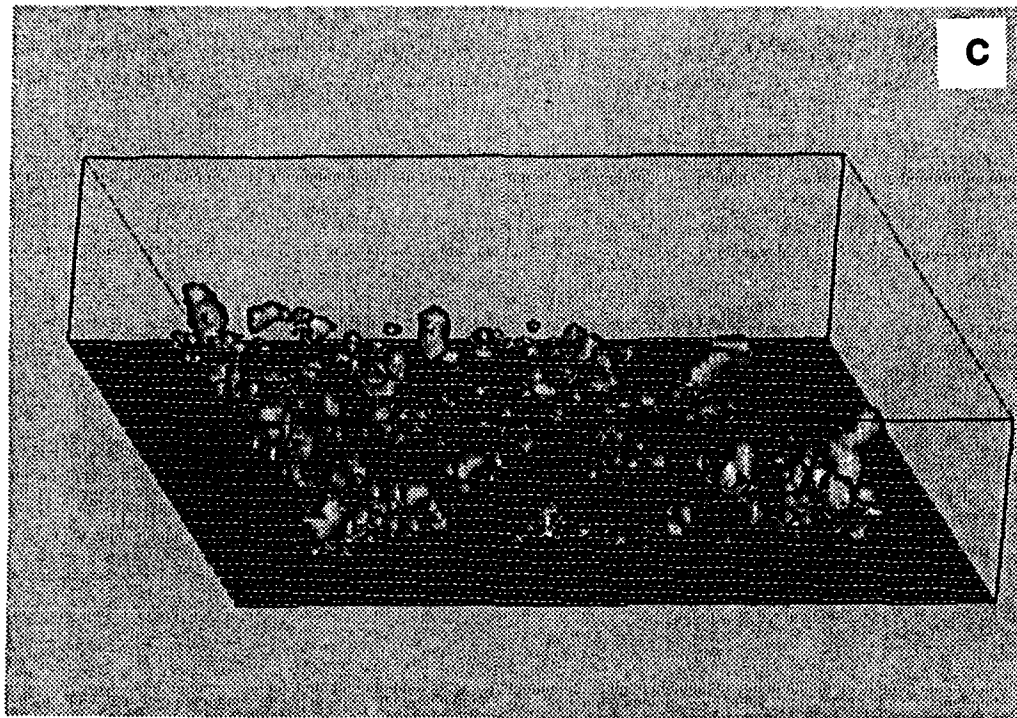
Figure 4 continued

(Figure 4e - following page in color)

RUN39   WMAX

TIME (MIN)

RUN39   RRF

TIME (MIN)
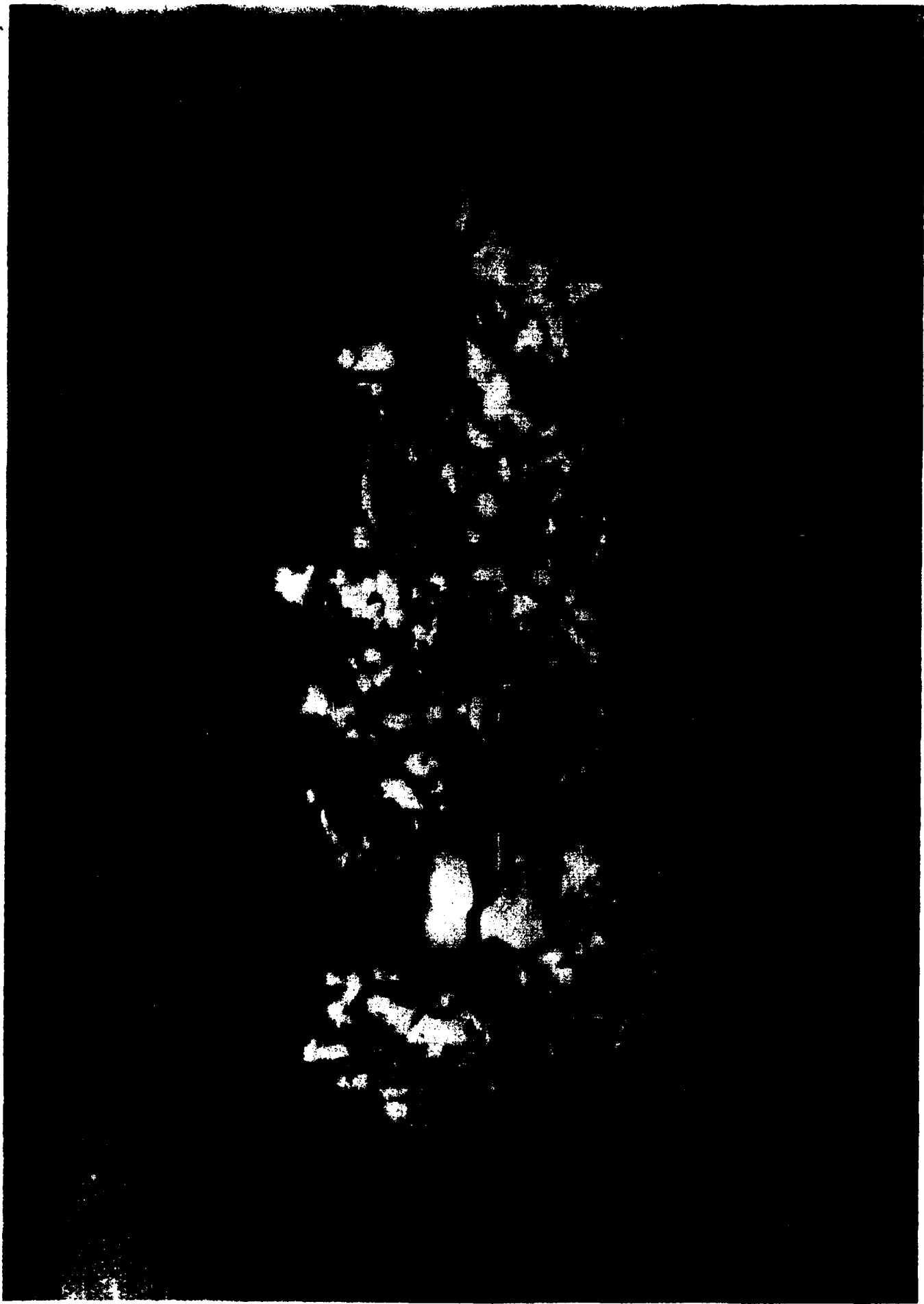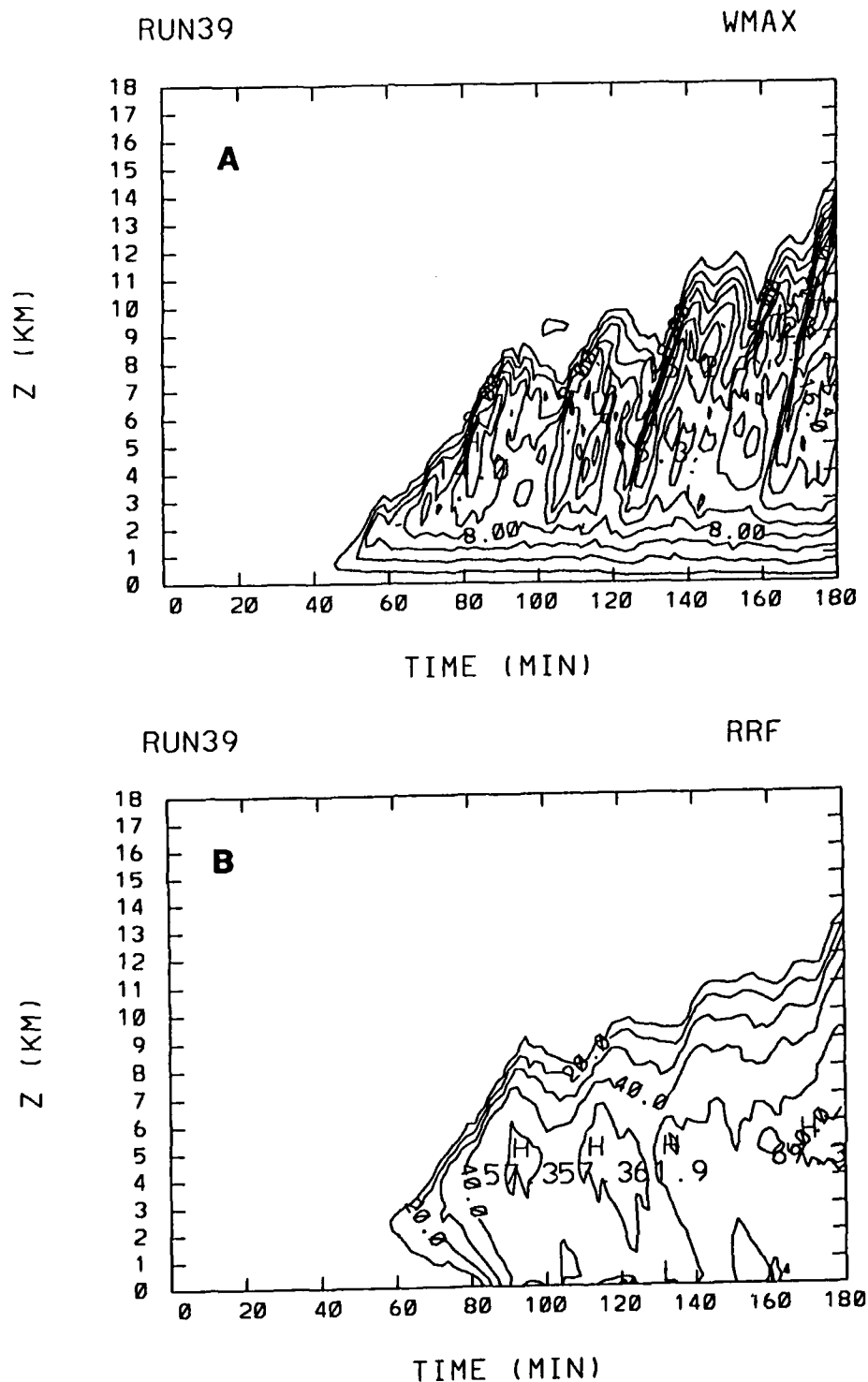
Figure 5 Time versus height contours for (a) maximum upward vertical velocity (m s⁻¹), and (b) maximum radar reflectivity (dBZ). Contour intervals are (a) 2 m s⁻¹ and (b) 10 dBZ.
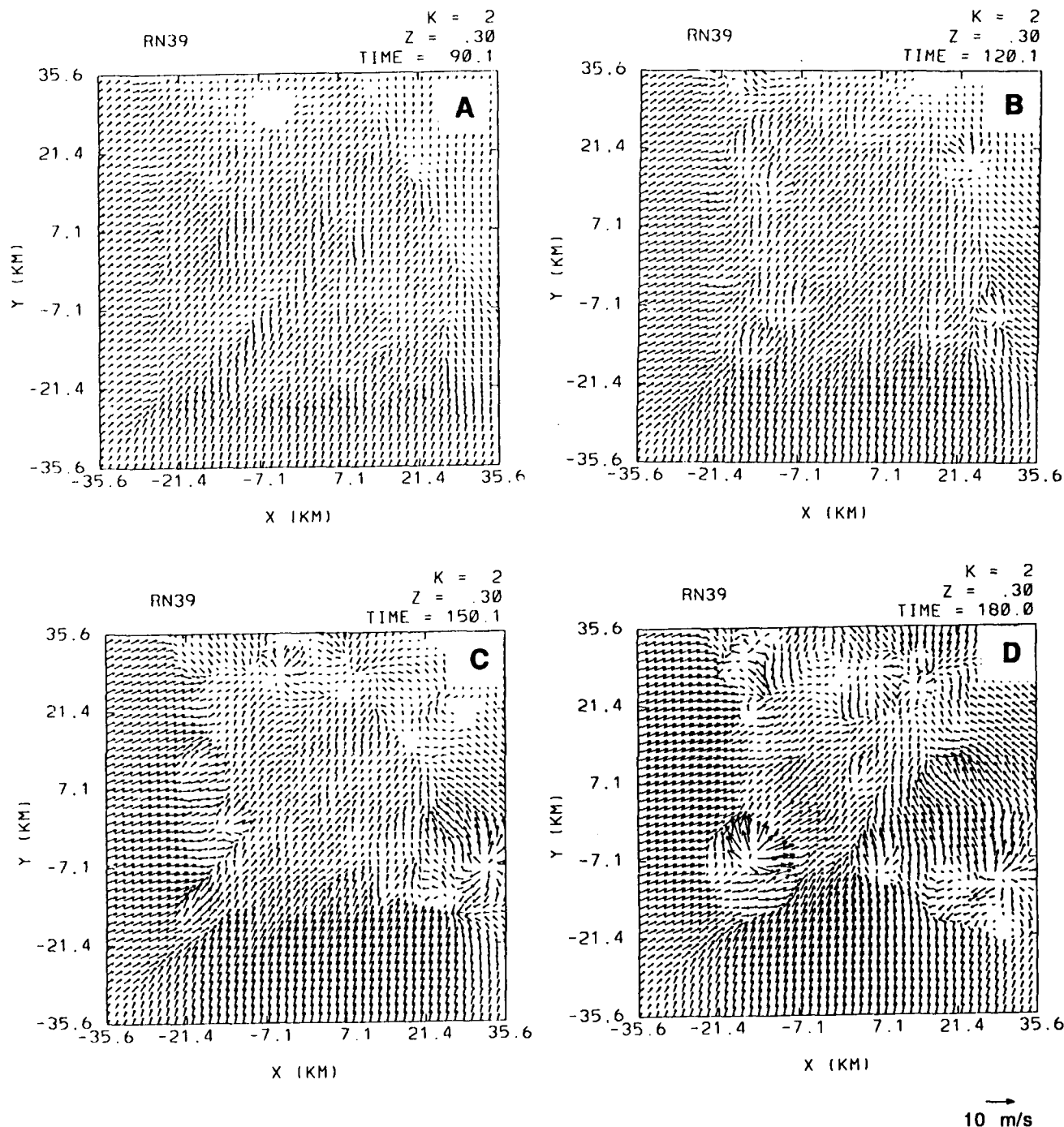
Figure 6 Model simulated low-level wind vector field at (a) 90 min, (b) 120 min, (c) 150 min and (d) 180 min. Height above the ground is 300 m.
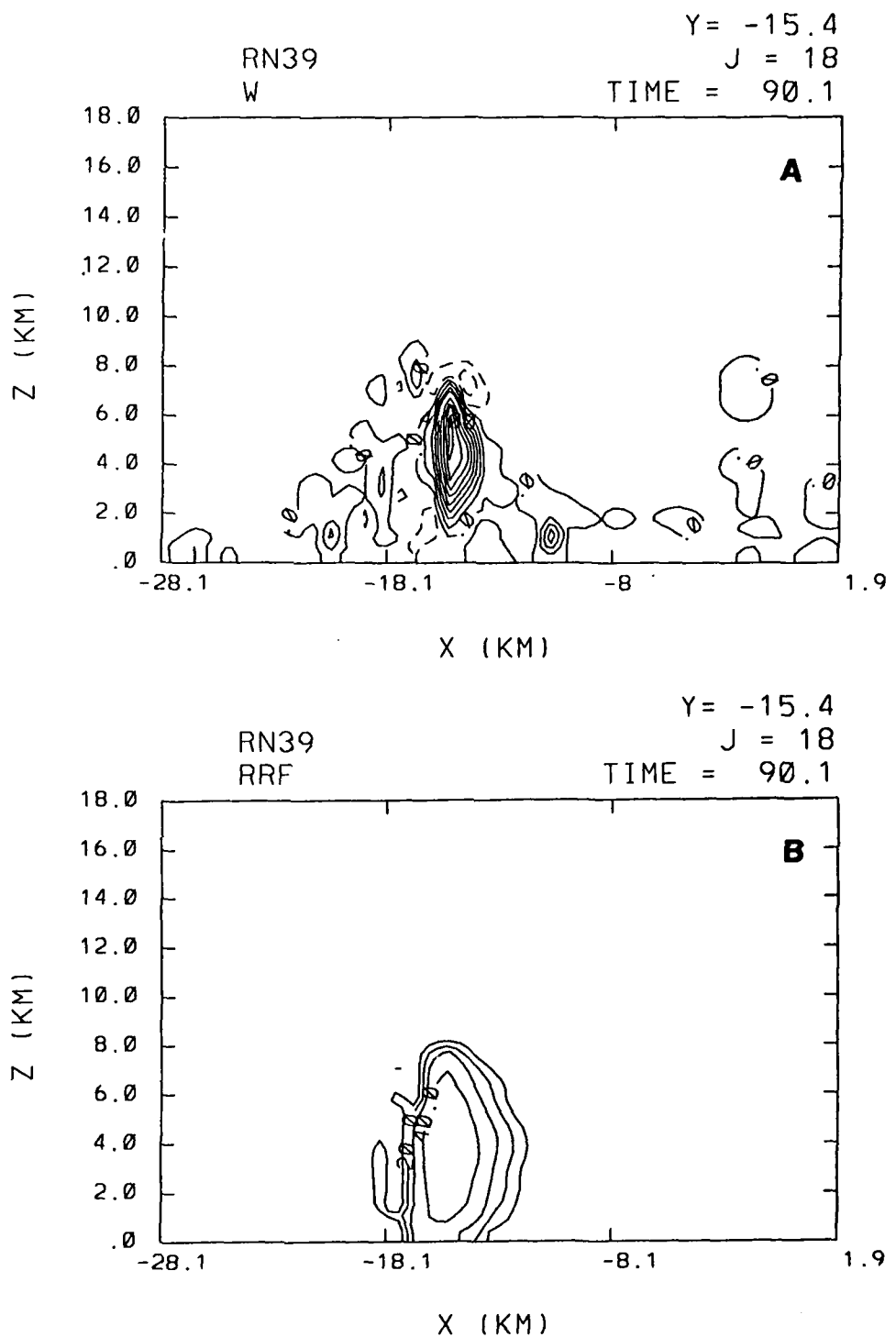
Figure 7 Vertical slices of simulated (a) vertical velocity and (b) radar reflectivity at 90 min over a 30 km subarea in the northwest quadrant of the domain. Contour intervals are (a) 1 m s^{-1} and (b) 10 dBZ.
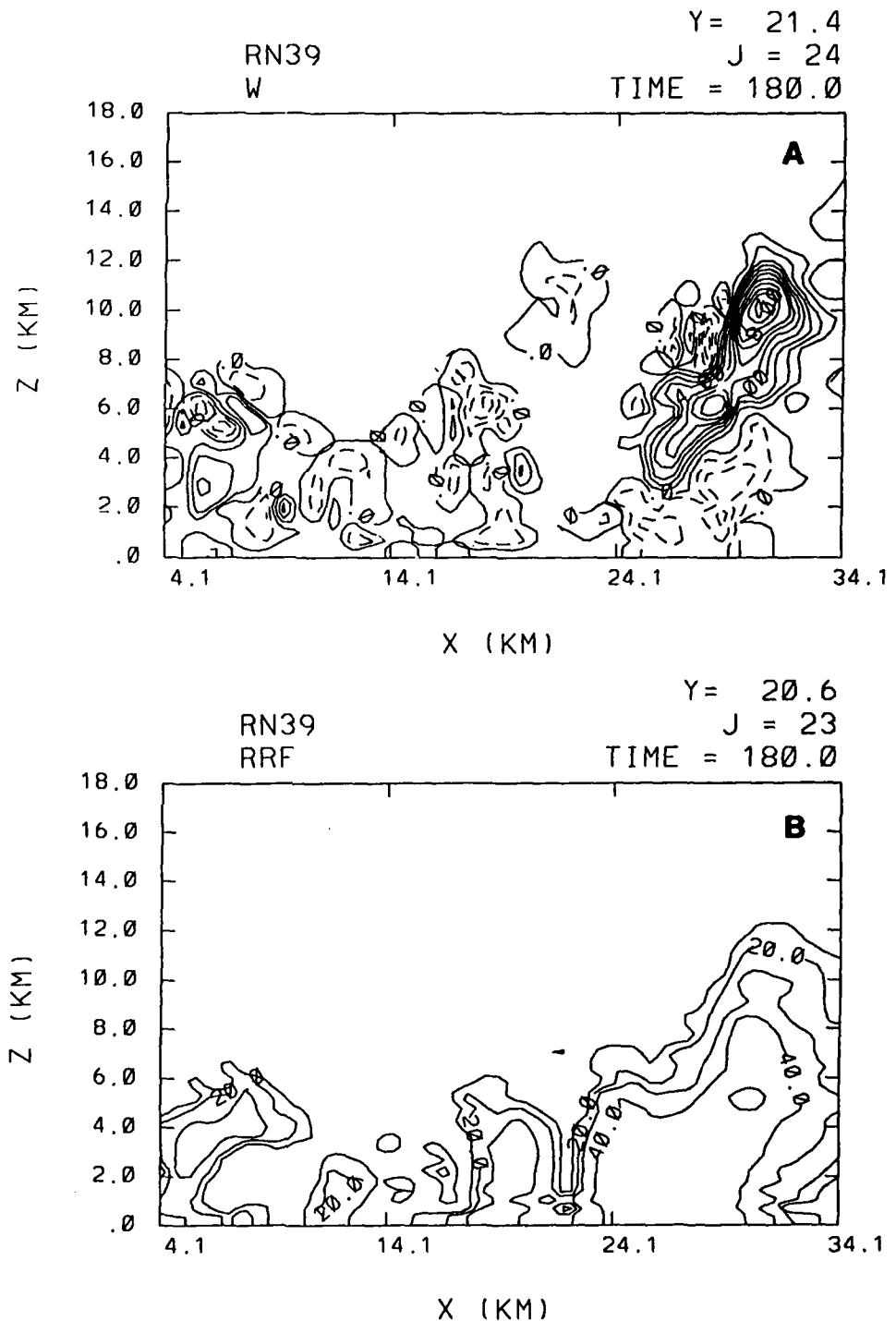
Figure 8 Vertical slices of simulated (a) vertical velocity and (b) radar reflectivity at 180 min over a 30 km subarea in the southeast quadrant of the domain. Contour intervals are (a) 1 m s^{-1} and (b) 10 dBZ.
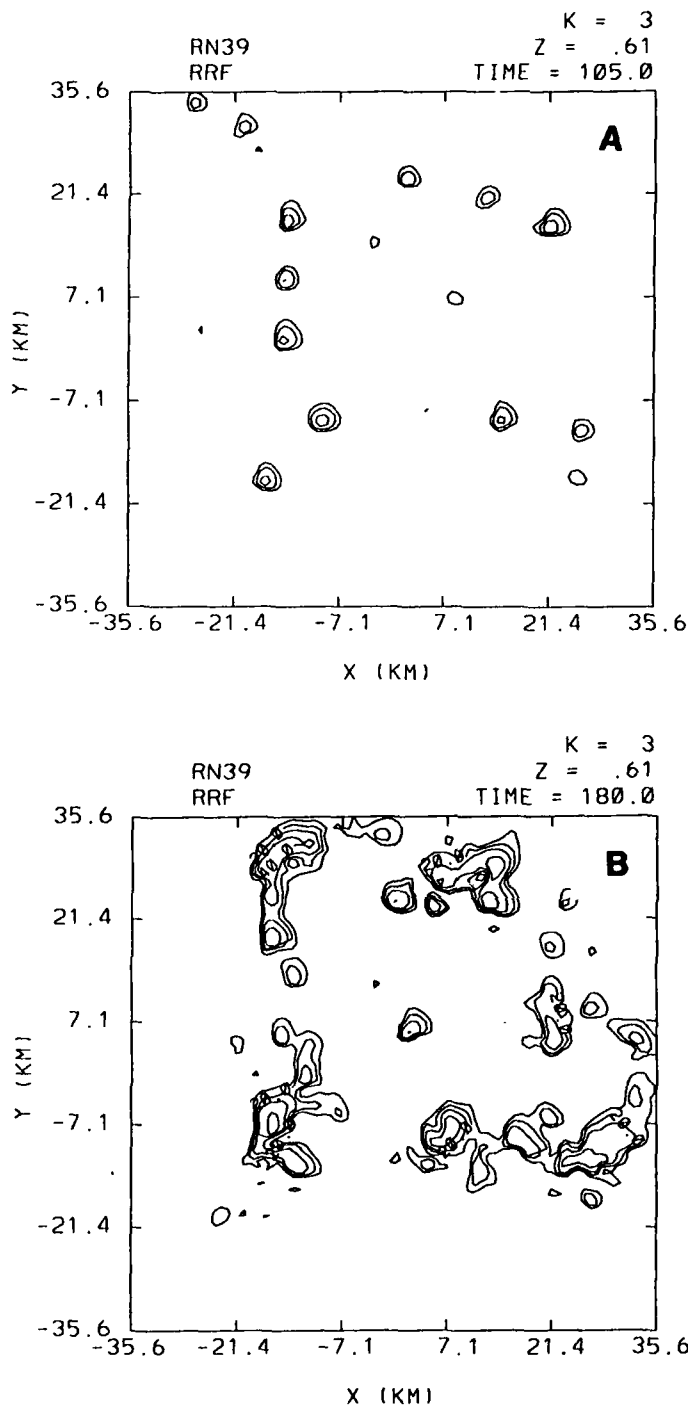
Figure 9 Horizontal slice of simulated low-level radar reflectivity over the entire domain at (a) 105 min and (b) 180 min. Contour interval is 10 dBZ.

4. Diagnostic And Statistical Analysis Of Model Results

In the following section, cloud model results will be examined from a different perspective, with the purpose of finding mesoscale indications of convective occurrence. Fig. 10 shows the contoured field of accumulated precipitation in two intervals, 90-120 minutes and 135-165 minutes. Also shown is an 8 x 8 grid of 8.25 km boxes employed in the mesoscale analysis.

4.1 Performance of existing mesoscale convective schemes

Fritsch and Chappell (1980) devised a convective parameterization scheme which was based on an equilibrium type of closure assumption (Frank, 1983). Once potential buoyant energy in the form of vertical instability is made available, convection will occur in a meso-β area at a rate which will remove a given percentage of the available buoyant energy (ABE) within a time period ranging between about 30 minutes and one hour. An understanding of the exact criteria used by the scheme for the initiation of convection is important. The scheme will allow convection to occur if *both* of the following conditions are met:

a. A parcel (anywhere in the lowest 300 mb of the atmosphere) lifted to its lifting condensation level (LCL) is warmer than its environment. A temperature perturbation which depends on the sign and intensity of the environmental vertical velocity at the LCL is added before the check for buoyancy.

b. A one-dimensional cloud model can then build a cloud which is at least 300 mb deep with an initial impulse of 1 m s^{-1} at cloud base.

Strictly speaking, this scheme would allow convection to occur with only an unstable enough sounding, even in the absence of any mesoscale convergence, unlike most other schemes which require convergence of some kind. However, a meso-β sounding is rarely absolutely unstable, and in practice, a positive temperature perturbation provided by upward grid scale vertical motion (implying low level convergence) is necessary.

THREAT and BIAS scores for the Fritsch-Chappell scheme are shown in Fig. 11. These were calculated by applying the full scheme to each grid point of the 8 x 8, 8.25 km averaged dataset at each 15 minute time level from 75 to 135 minutes into the simulation, and comparing the schemes prediction of convection (yes/no) to the accumulated rainfall (yes if greater than 0.1 mm averaged over the 8.25 km box) in the same box over the following 30 min. This is approximately the way the scheme is applied in a mesoscale model. In addition, the scheme's prediction is checked against accumulated rainfall for later 30 minute periods.

The THREAT scores generally range from 0.2 to 0.3, which are fairly good, but the scheme greatly overpredicts convection at every time level, as shown by the BIAS scores exceeding 3.0, meaning that the scheme predicts three times the actual amount (number of boxes) of convection. Fig. 12 compares the distribution of convection predicted by the scheme to the actual distribution. The major problem is that the entire domain is convectively unstable by the Fritsch-Chappell criteria (devised for a larger grid size), and the only places where convection is not predicted is probably where the grid scale vertical velocity at the LCL is downward, resulting in the addition of a negative temperature perturbation to the parcel temperature.

Perhaps unsurprisingly, the Fritsch-Chappell scheme performs poorly on the TASS-derived datasets, generally overpredicting convection and showing little distinguishing power between convective and non-convective areas. First, the scheme was designed for a specific grid spacing (25 km) which is larger than possible for the TASS-averaged data because of the limited TASS domain. Second, the scheme makes some assumptions which are very scale-dependent, including the assumption that convective updrafts, downdrafts, and the compensating environmental vertical motion (primarily subsidence) all occur in one mesoscale grid box. Such an assumption is clearly invalid for a grid size of 8.25 km. It is considered to be a fundamental weakness of the scheme that it is tied to one particular grid spacing. Any improved scheme needs to make assumptions which are valid over a range of mesoscale lengths.

Anthes (1977) presented a cumulus parameterization scheme which is based on earlier work by Kuo (1965, 1974). This scheme uses vertically integrated moisture convergence to parameterize the amount of condensation in a column. The moisture convergence is given by

$$MCON = -\frac{1}{g}\int_0^{P_s} \overline{\nabla} \cdot \overline{V} q \, dp ,$$

$$(4.1)$$

where g is the acceleration due to gravity, V is horizontal velocity, q is water vapor mixing ratio, and the integral is taken over the depth of the column by pressure. The condensational heating represented by a fraction of this moisture convergence (the rest is stored in the column) is then distributed in the vertical by a one-dimensional cloud model. For convection to occur in the Kuo scheme, moisture convergence above a threshold amount must occur, and the atmosphere must be unstable enough to build a deep cloud. Although the scheme was intended for large scale models (100 km grid spacing and above), it has been applied in models with a wide range of grid sizes, from the global to the meso-β-scale.

Instead of directly applying the complete Kuo scheme to the TASS-averaged data, the fundamental closure assumption of the scheme has been examined, that moisture convergence is instantaneously related to convective precipitation. Fig. 13 shows the correlation between moisture convergence and accumulated rainfall for the 64 8.25 km boxes averaged from 105 to 135 min. In general, the points with the largest rainfall have positive moisture convergence, although some non-convective points also do. Fig. 14 qualitatively compares the distributions of moisture convergence and rainfall from 90-120 min, shortly after precipitation begins. The circular pattern of convergence caused by the heat island effect has already emerged, and the pattern of rainfall is beginning to become organized on the mesoscale. Fig. 15 compares the same two fields from 135-165 min. The moisture convergence pattern is stronger and the convective rainfall seems to follow more closely the intensity of the moisture convergence, although the two maxima are sometimes offset by one grid point, something which is not revealed by the purely statistical approach (Fig. 13).

In Fig. 16, the evolution of moisture convergence and rainfall in time is shown for the six 8.25 km boxes which had the most rainfall from 135-165 min. For most of these points, increases in moisture convergence seem to be well correlated with convective rainfall. At point (6,3), 2 mm of rain in the absence of significant moisture convergence may be due to initiation from outflow boundaries from earlier cells; this convergence may be

subgrid scale and not resolved at 8.25 km.

THREAT and BIAS scores were calculated using the simple criterion that 8.25 km grid boxes which have a 30 minute average moisture convergence which is positive will be considered convective. Fig. 17 shows that the THREAT scores of about 0.2 to 0.4 were obtained with this simple formulation, along with reasonable BIAS scores of 1.0 to 2.0. The earliest BIAS scores are very large, as all of the methods predicted convection to begin before it did. At later times, the THREAT scores were high when moisture convergence is compared to rainfall over the same time interval, suggesting that the Kuo instantaneous relationship may be valid, even at grid sizes as small as 8.25 km. Fig 12c shows the areas of positive moisture convergence averaged from 105 to 135 min; the circular pattern of convergence related to the inflow from the boundaries (heat island effect) is prominent.

4.2   *Correlations of Rainfall with Other Convective Parameters*

The basic combination of parameters used in existing parameterization schemes involves some measures of stability and either convergence or vertical motion, both taken over a mesoscale area. For this run, forced only by differential surface heating, combinations of these averaged parameters generally produced very little correlation. In particular, mesoscale CAPE as a measure of instability was not at all a good indicator of the likely presence of convection. Fig. 18 shows the correlation of CAPE to rainfall at 105 to 135 min. Convection occurs in mesoscale boxes with both low and high CAPE values with no discernible trend. What seems to be happening is that in the first 90 minutes of the simulation, surface sensible heating removes the initial negative sounding area, generally increasing the CAPE. Later on, cool downdrafts spread out in the lowest level, significantly reducing CAPE in those areas. But neither the initial formation of convection from differential surface heating, nor the later development of mesoscale convergence is accompanied by any mesoscale signal in the CAPE field which can be related to convection. It is concluded that vertical instability is a necessary, but not a sufficient condition for convection, i.e. that vertical instability may indicate the ability of an area to respond to vertical motion with convective initiation, but it cannot distinguish which areas will become convective in a generally unstable

region. Both Frank (1983) and Fritsch and Chappell (1980) make essentially the same point.

Vertical velocity calculated by the kinematic method (from the continuity equation) on the 8.25 km grid shows a weak correlation with rainfall, but the cloud model vertical velocity at 700 mb, when averaged to 8.25 km, shows a stronger correlation (Fig. 19). The prognostic value of the TASS-averaged vertical velocity is dubious, however, since the average includes the actual updraft values, which is not knowable on the mesoscale.

Some subgrid scale variables correlate well with convection. In runs with light winds, the standard deviation of the sensible heat flux (a measure of the subgrid variability of the surface) correlates well with convective initiation. The variable surface leads to subgrid scale convergence and then to convection, when uncomplicated by advection. It is important to note that the *variability* of surface heating is more significant in this case than the *average* surface heating, showing that the convergence (and presumably destabilization) at the subgrid scale is more effective than area-averaged destabilization. In the early part of this simulation, convection forms near areas with strong differential heating, but later the influence of the surface heating pattern is not strong, as shown by the standard deviation of the sensible heat flux at 105 to 135 minutes (Fig. 20). The standard deviation of the level 1 temperature generally correlates well with convection, although at later times the interpretation of the relationship becomes complicated by the presence of outflow boundaries with strong temperature gradients, which represent both the potential for new initiation and the existence of earlier convection.

Of the seventeen parameters listed in Table 2, the one which seems to correlate best to convective rainfall is the maximum subgrid scale convergence. The maximum subgrid scale convergence in an 8.25 km box is the largest value of convergence on the TASS grid (750 m resolution) which falls within that box. Fig. 21 shows the relationship during the interval 135-165 minutes. Almost all of the convergence associated with the initial differential surface heating occurs on small scales, and is therefore captured by that parameter. The relationship gets stronger with time, so it seems that the area-averaged convergence and the subgrid

convergence are also well correlated. Based on Fig. 21, another simple criterion for convection was formulated, that convection is predicted to occur at points where the maximum subgrid level 1 convergence is greater than or equal to .005 s^{-1}. Fig. 22 shows the THREAT and BIAS scores for this method. The BIAS scores are very good, and the THREAT scores improve in the later part of the run, when they reach 0.5, greater than for the other methods. Interesting is that after 120 minutes, the value of the forecasts increase with time, suggesting predictive ability beyond the period during which the convergence was calculated. Fig. 12d shows the spatial correlation with convection.
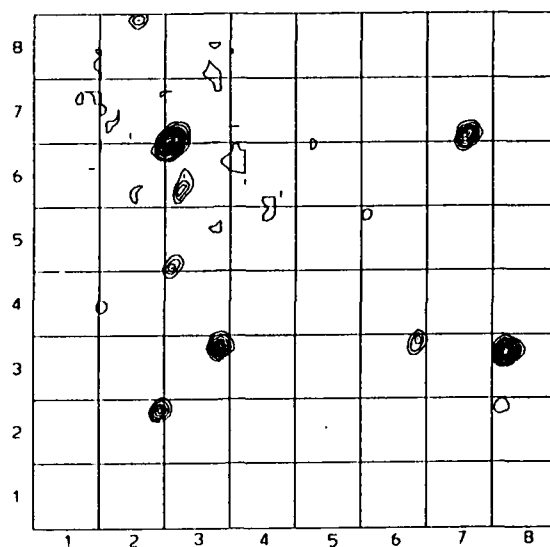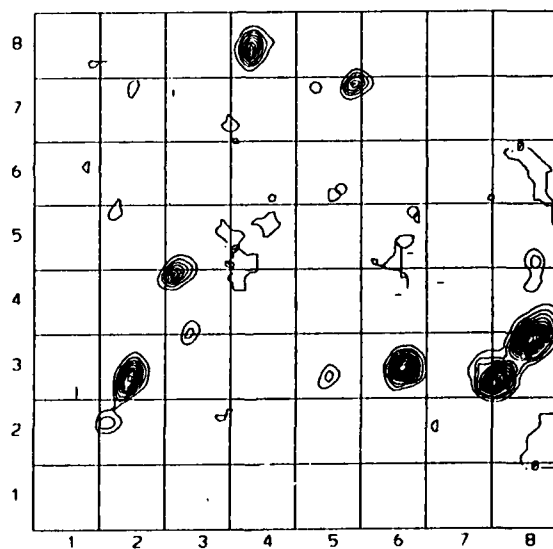
Figure 10 Accumulated precipitation field taken between: (a) 90-120 min, and (b) 135-165 min. The contour interval is 1 mm for both plots. The grid boxes shown are 8.25 km in size; the locations are indexed the way they are referenced in the text.
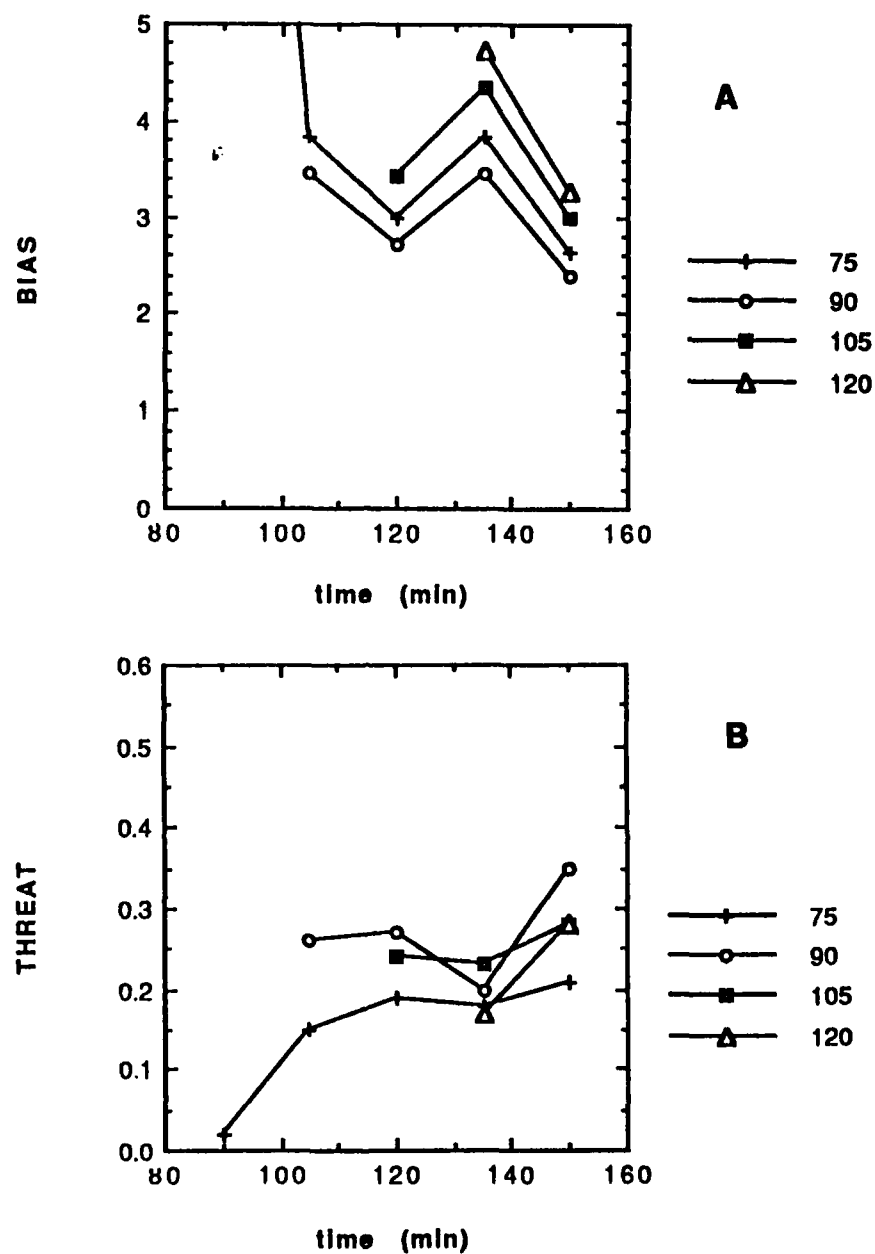
Figure 11 (a) THREAT and (b) BIAS scores for the Fritsch-Chappell scheme. Each curve represents one Fritsch-Chappell run at the beginning time (leftmost point on the curve). Points on the same curve later in time show how the initial prediction compares against progressively later rainfall distributions.
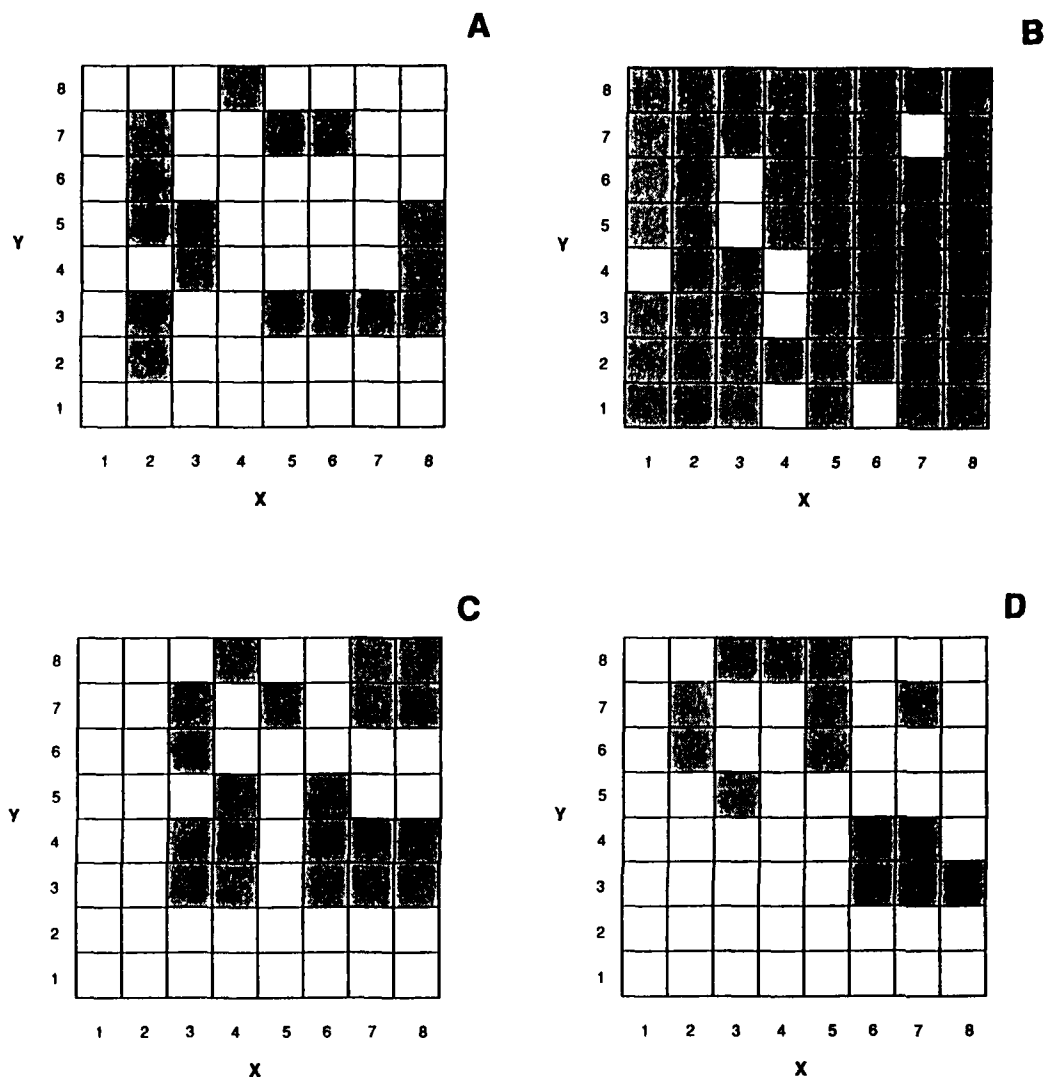
Figure 12 Pattern of mesoscale grid boxes in which the rainfall exceeds 0.1 mm (shaded) from 105 to 135 min: (a) produced by the cloud model, (b) as predicted by the Fritsch-Chappell scheme, (c) as predicted by the moisture convergence criterion, and (d) as predicted by the level 1 subgrid convergence criterion. For the location of the boxes on the TASS grid, see Fig. 10.
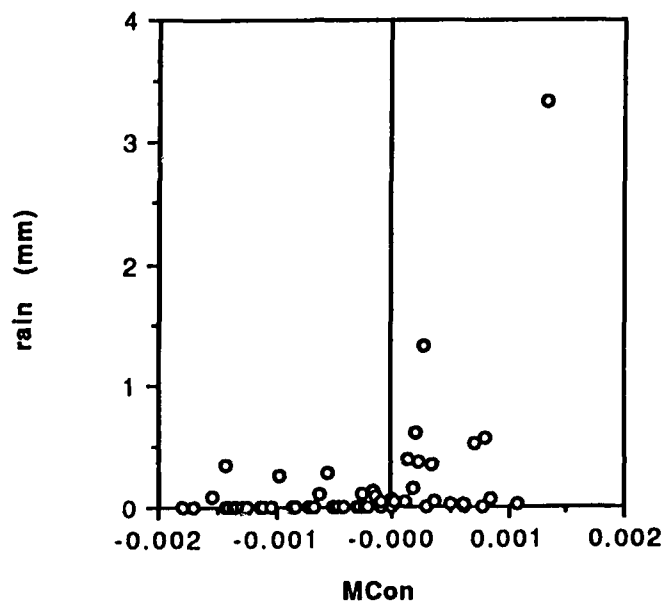
Figure 13 Scatter plot of mesoscale (8.25 km) column moisture convergence vs. accumulated rainfall in the interval from 105-135 min.
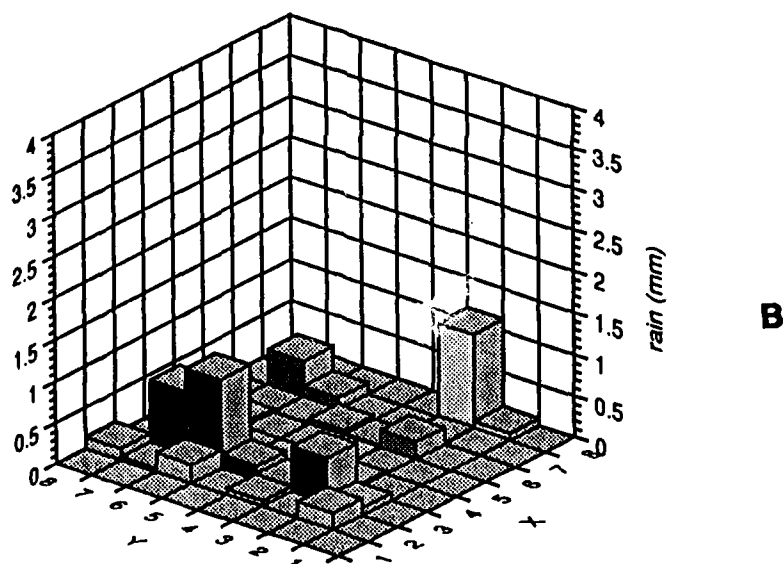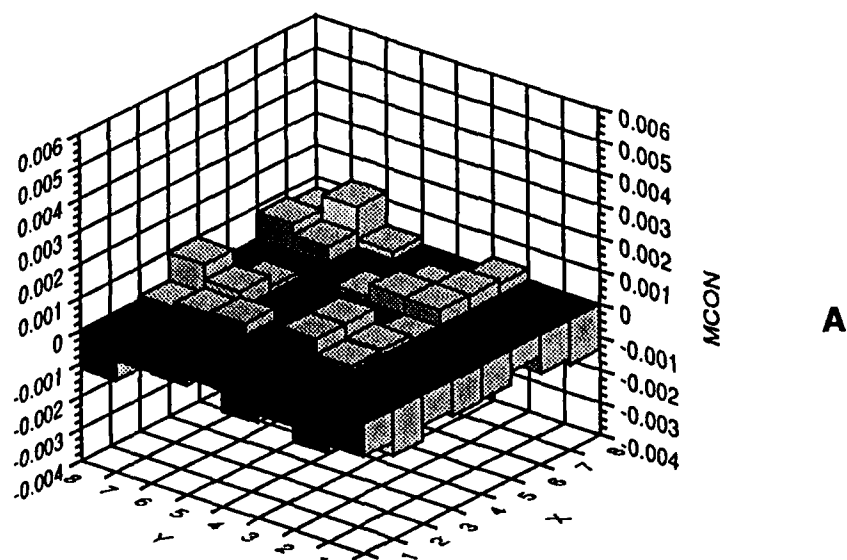
Figure 14 Spatial patterns of (a) moisture convergence and (b) accumulated rainfall in the interval from 90-120 min. The view is looking from the southwest.
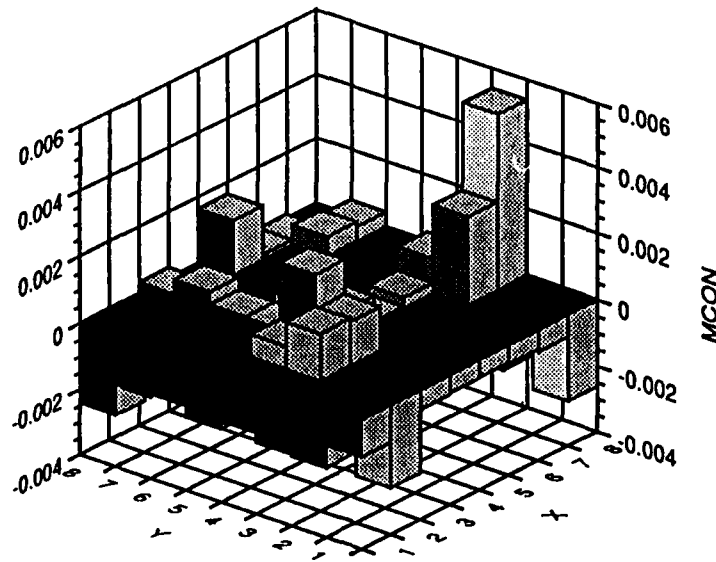
A
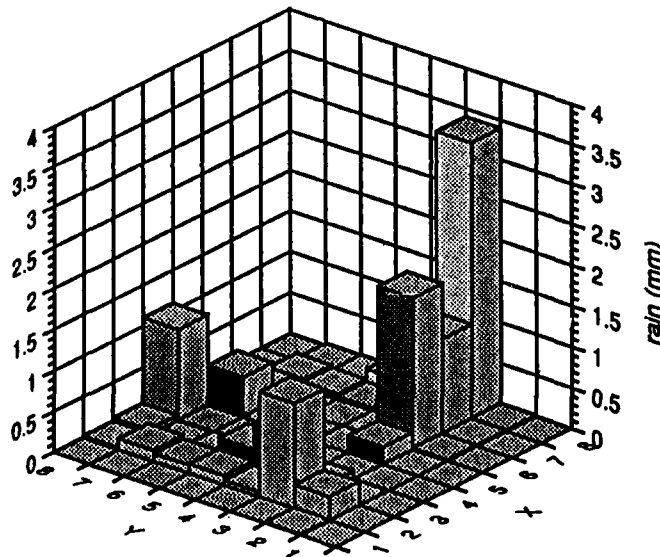
B

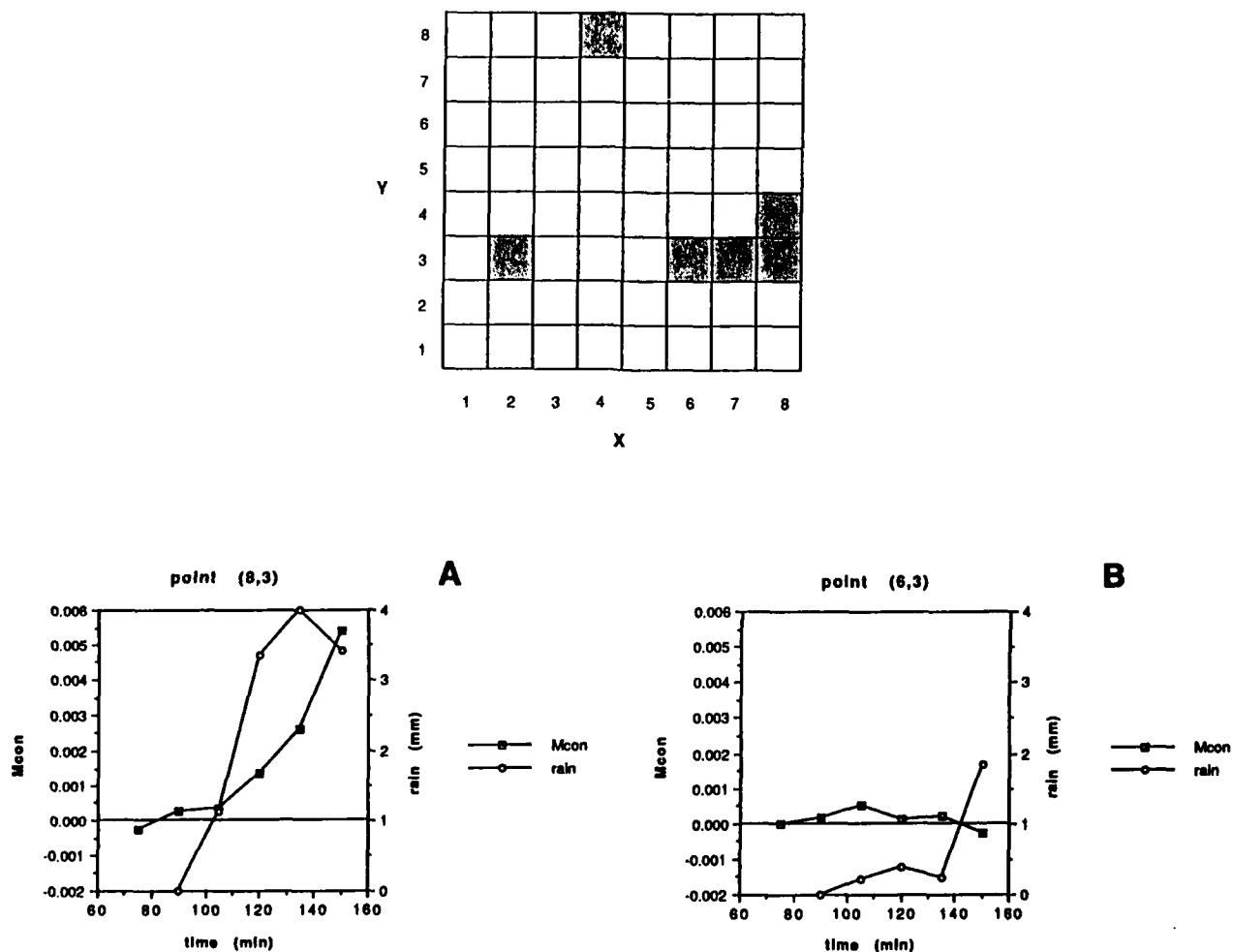**Figure 15** Same as Fig. 14 except in the interval from 135 to 165 min.

Figure 16 The evolution of moisture convergence and rainfall with time at the six mesoscale grid boxes with the most rainfall from 135 to 165 min. The shaded grid shows the location of the six boxes.
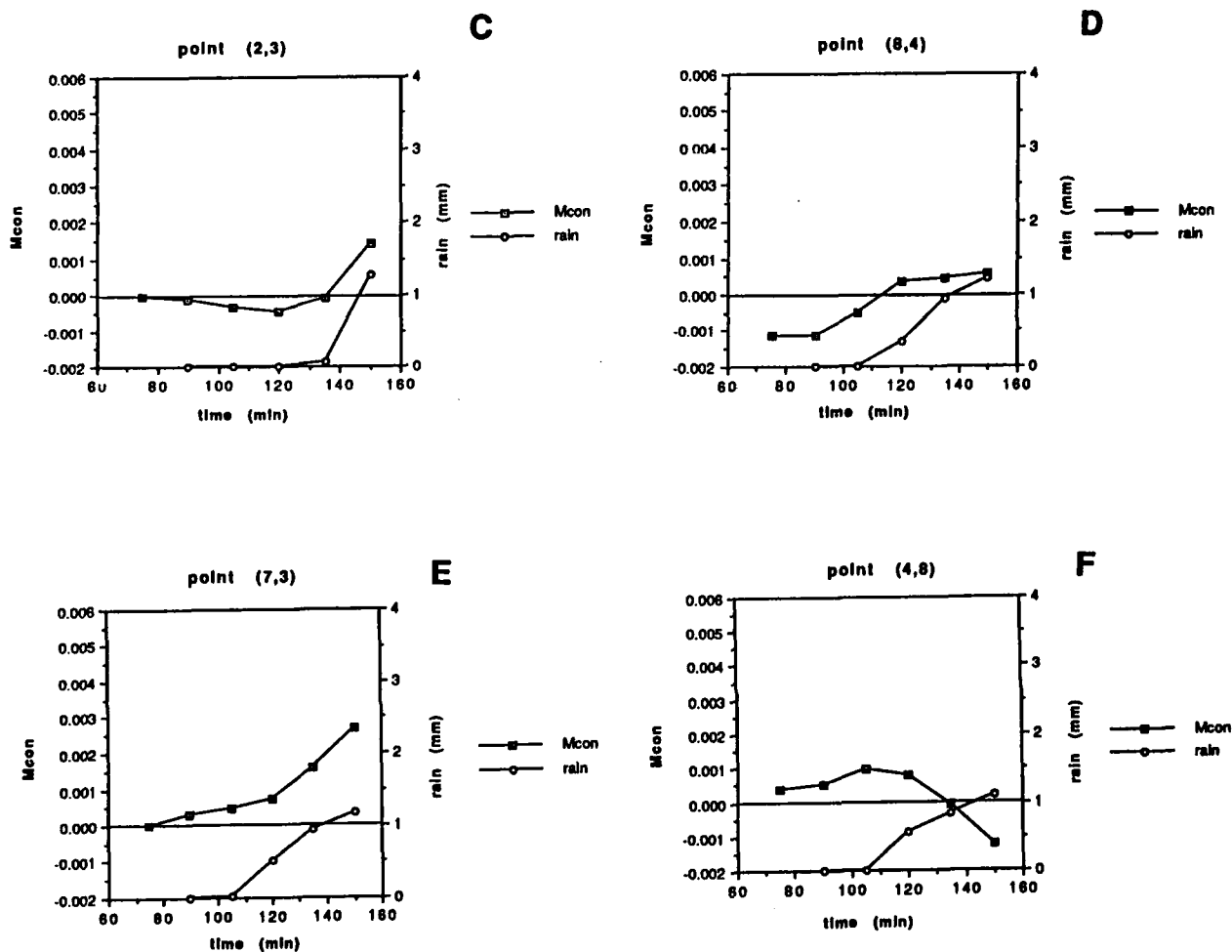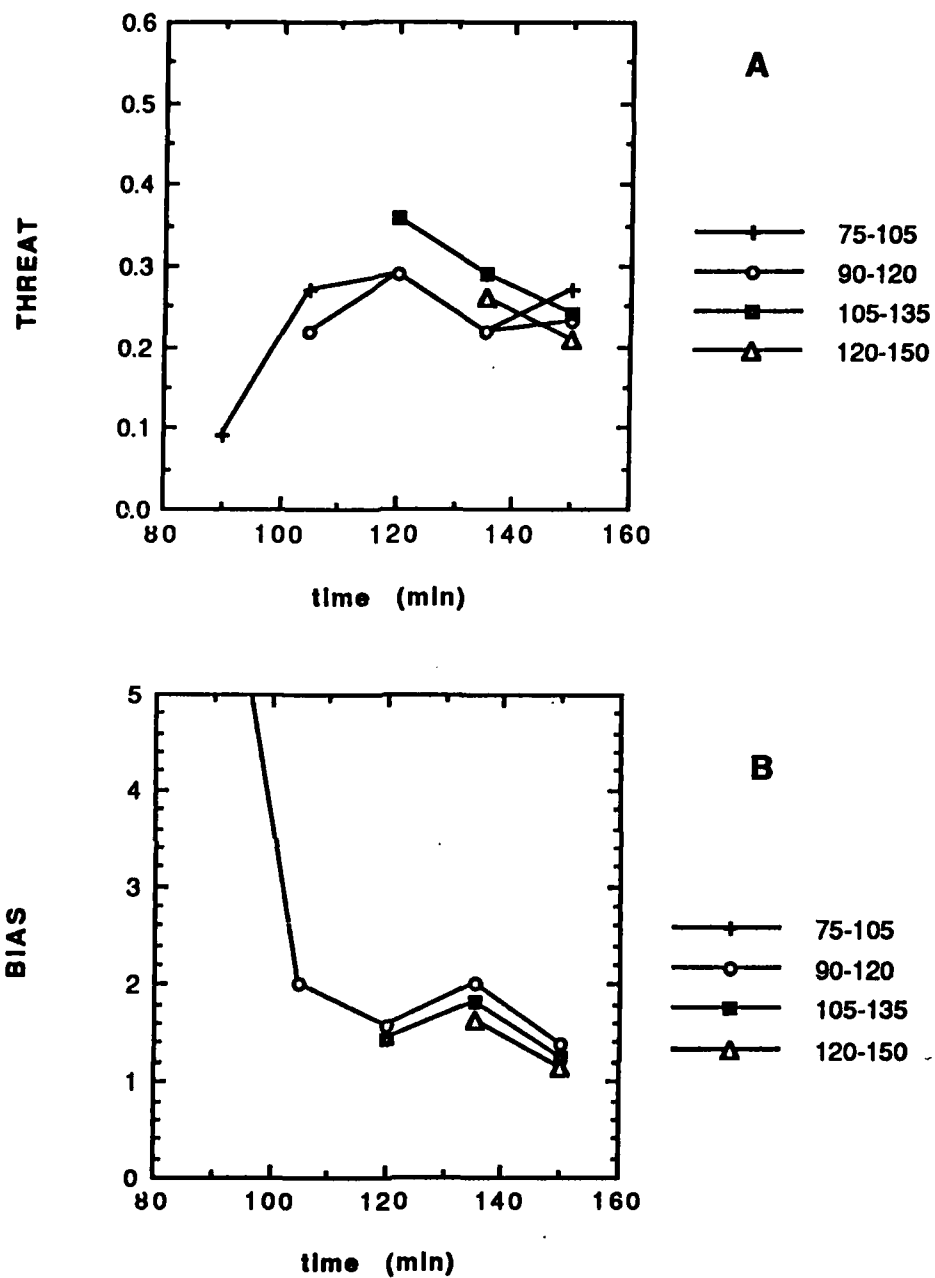
Figure 16 Continued.

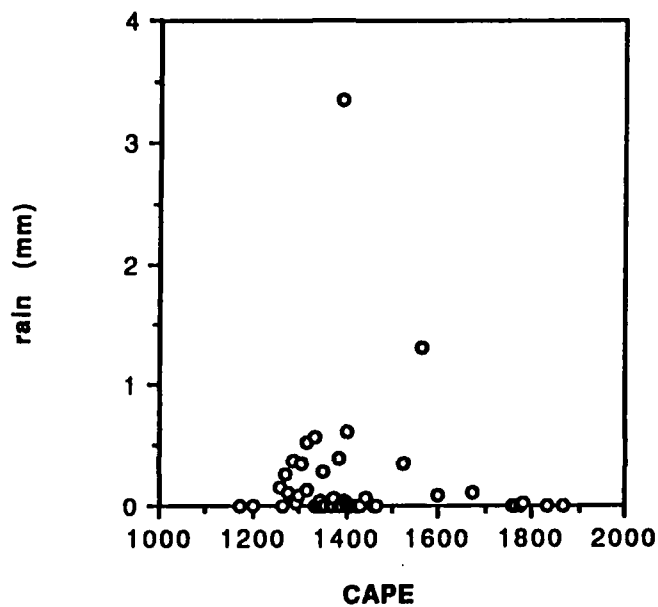**Figure 17** As in Fig. 11 except using the moisture convergence convective criterion.

Figure 18 Scatter plot of mesoscale Convective Available Potential Energy (CAPE, J kg^{-1}) vs rainfall in the interval from 105 to 135 min.
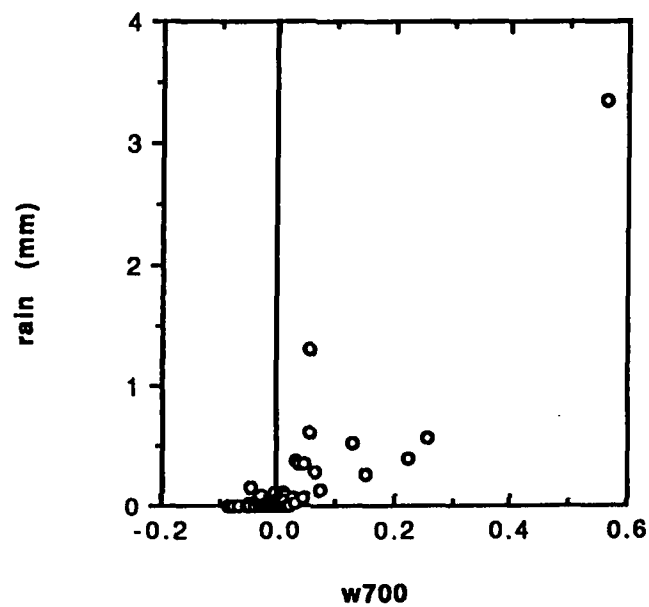
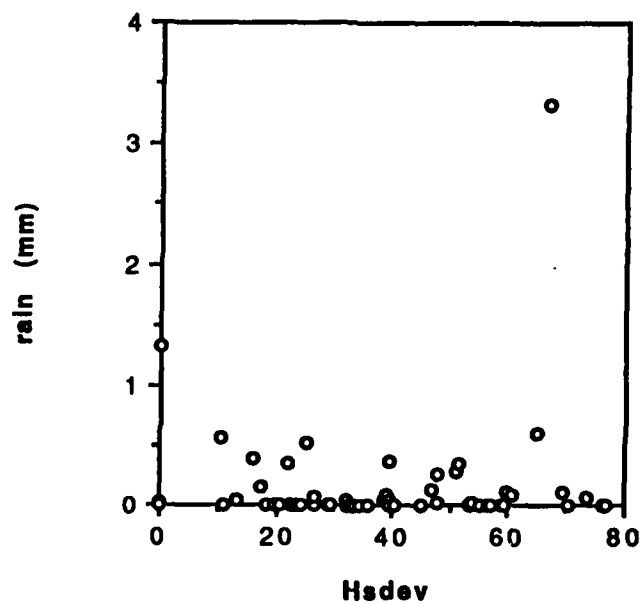**Figure 19** As in Fig. 18 except for average vertical velocity at 700 mb $(m\ s^{-1})$.

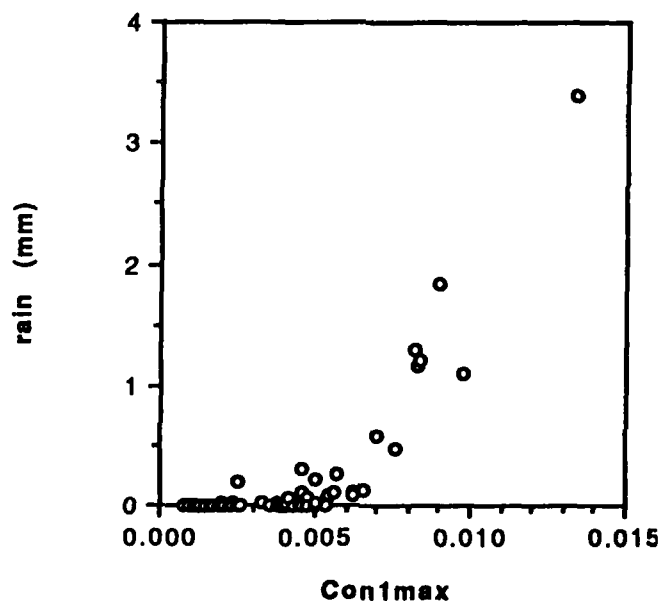**Figure 20** As in Fig. 18 except for the standard deviation of initial sensible heat flux (W m^{-2}).

Figure 21 As in Fig. 18 except for the maximum subgrid level 1 convergence (s⁻¹) at 135-165 min.
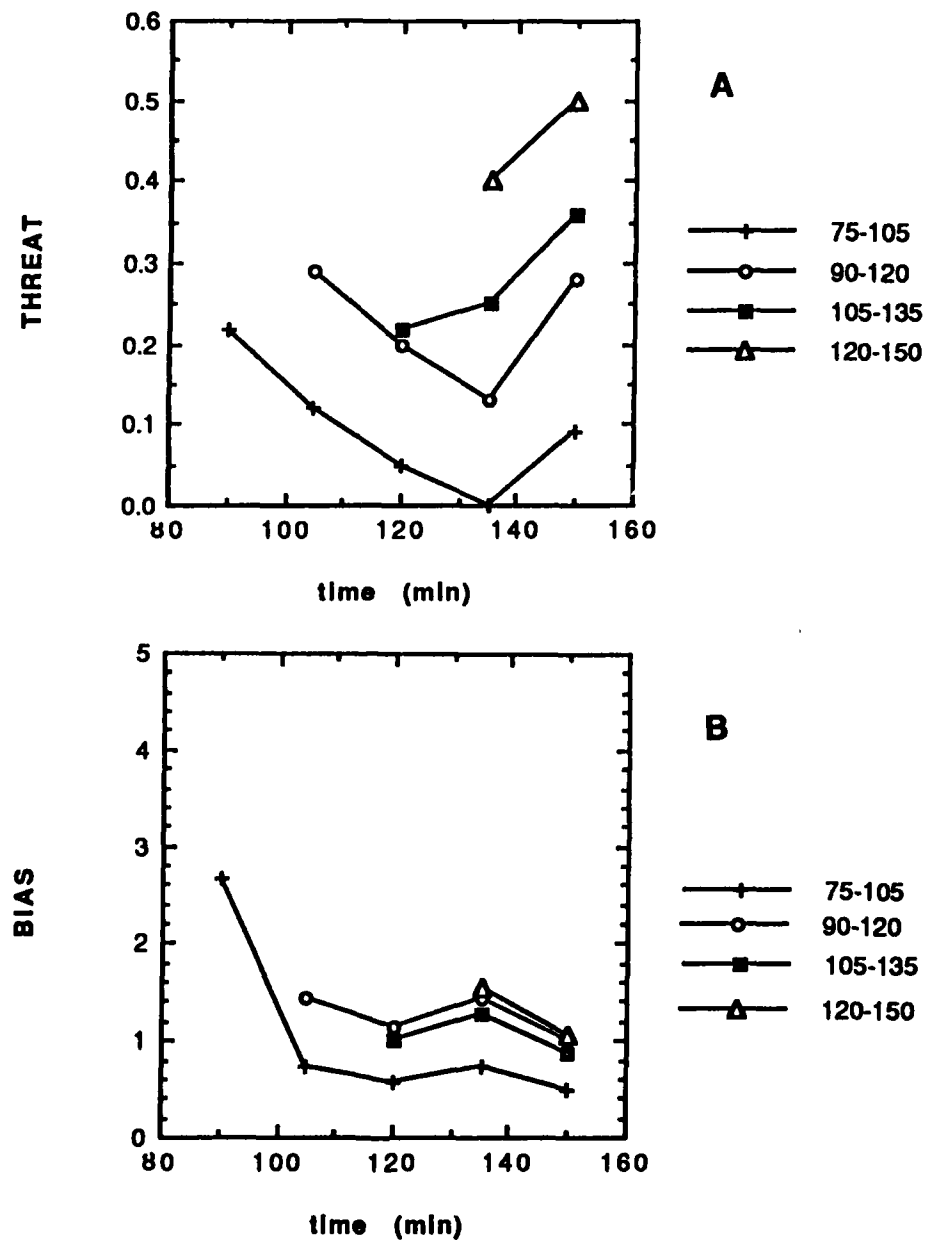
Figure 22 As in Fig. 11 except using the level 1 subgrid convergence criterion.

5. Summary And Suggestions For Phase II Research

The first major objective of this work was to demonstrate that a cloud modeling approach is feasible for the study of convective initiation. The TASS cloud model has proven to be a useful tool for recreating and studying a complex pattern of convection in order to search for signals which define the location and timing of the convection. This case provided a simplified first step toward the future of initializing the cloud model with a fully three-dimensional mesoscale dataset including both mesoscale and complex surface forcing. Even with no horizontal variation in the initial environment, realistic convection was organized on the small scale and on the mesoscale.

The second major objective was to show relationships between mesoscale variables which can effectively diagnose or predict the initiation of convection from differential surface heating. The Fritsch-Chappell scheme did a poor job of predicting convective occurrence, although the fact that it was formulated for a larger (25 km) grid spacing than the 8.25 km used in this study makes conclusions regarding its closure assumptions difficult. On the other hand, the Kuo-type closure assumption proved to be surprisingly good. Moisture convergence was fairly well correlated with convective precipitation when both were averaged over a 30 minute time interval. That relationship was successful at 8.25 km in spite of the fact that the scheme was originally intended for use in meso-α or larger scale models.

In lieu of directly measuring small scale variables, it is believed necessary to effectively estimate subgrid scale variables in the many cases when surface-based small scale forcing is important. Subgrid convergence correlated very well with convective precipitation in this simulation. Essentially all of the convection was forced by differential surface heating; the earliest convection from sensible heat gradients within the grid, and gradually building domain scale convergence generated by the discontinuity in surface fluxes at the lateral boundaries. *These results encourage the idea that a simple mesoscale variable like moisture convergence, in combination with an inferred measure of subgrid scale forcing, can result in significantly improved mesoscale thunderstorm forecasts.*

The next step in the use of the cloud model approach should be to verify that given the surface characteristics and the mesoscale environment of a particular case, the model can reproduce the location and at least roughly the timing of the actual convection that is observed. In order to do that, an improved lateral boundary condition scheme must be implemented in the TASS model to prevent the formation of artificial gradients at the boundaries. Also, the specification of surface heat fluxes should be replaced with a set of interactive equations (a surface energy budget) which would allow realistic evolution of fluxes with time. It is believed that the analysis of complex cloud model results represents the best way to develop a more complete understanding of convective initiation and evolution on a range of scales, with the goal of a much improved parameterization scheme suitable for use in operational mesoscale forecasting.

6. REFERENCES

Anthes, R.A., 1977: A cumulus parameterization scheme utilizing a on-dimensional cloud model. *Mon. Wea. Rev.*, **105**, 270-286.

Balaji, V. and T.L. Clark, 1988: Scale selection in locally forced convective fields and the initiation of deep cumulus. *J. Atmos. Sci.*, **45**, 3188-3211.

Chen, C.-H. and H.D. Orville, 1980: Effects of mesoscale convergence on cloud convection. *J. Appl. Meteor.*, **19**, 256-274.

Cooper, H.J., M. Garstang and J. Simpson, 1982: The diurnal interaction between convection and peninsular-scale forcing over South Florida. *Mon. Wea. Rev.*, **110**, 486-503.

Cunning, J.B. and M. DeMaria, 1986: An investigation of the development of mesoscale convective systems. Part I: Boundary layer interactions. *Mon. Wea. Rev.*, **114**, 5-24.

Cunning, J.B., M. DeMaria and H.W. Poor, 1986: An investigation of the development of cumulonimbus systems over south Florida. Part II: In-cloud structure. *Mon. Wea. Rev.*, **114**, 25-39.

Frank, W.M., 1983: The cumulus parameterization problem. *Mon. Wea. Rev.*, **111**, 1859-1871.

Frank, W.F. and C. Cohen, 1987: Simulation of tropical convective systems: Part I: A cumulus parameterization. *J. Atmos. Sci.*, **44**, 3787-3799.

Fritsch, J.M. and C.F. Chappell, 1980: Numerical prediction of convectively driven mesoscale pressure systems. Part I: Convective parameterization. *J. Atmos. Sci.*, **37**, 1722-1733.

Kuo, H.L., 1965: On formation and intensification of tropical cyclones through latent heat release by cumulus convection. *J. Atmos. Sci.*, **22**, 40-63.

_____, 1974: further studies of the parameterization of the influence of cumulus convection on large-scale flow. *J. Atmos. Sci.*, **31**, 1232-1240.

Kuo, Y.-H. and R.A. Anthes, 1984: Semiprognostic tests of Kuo-type cumulus parameterization schemes in an extratropical convective system. *Mon. Wea. Rev.*, **112**, 1498-1509.

Lin, Y.-L., R. D. Farley, and H. D. Orville, 1983: Bulk parameterization of the snow field in a cloud model, *J. Climate Appl. Meteor.*, **22**, 1065-1092.

Proctor, F.H., 1987a: The Terminal Area Simulation System. Volume I: Theoretical formulation, NASA CR-4046.

Proctor, F.H., 1987b: The Terminal Area Simulation System. Volume II: Verification Cases, NASA CR-4047.

Redelsperger, J.-L. and T.L. Clark, 1990: The initiation and horizontal scale selection of convection over gently sloping terrain. *J. Atmos. Sci.*, **47**, 516-541.

Rutledge, S. A. and P. V. Hobbs, 1983: The mesoscale and microscale structure and organization of clouds and precipitation in midlatitude cyclones. VIII: A model for the "seederfeeder" process in warm-frontal rainbands, *J. Atmos. Sci.*, **40**, 1185-1206.

Zhang, D.-L., E.-Y. Hsie and M.W. Moncrieff, 1988: A comparison of explicit and implicit predictions of convective and stratiform precipitating weather systems with a meso-β-scale numerical model. *Quart. J. Roy. Meteor. Soc.*, **114**, 31-60.

_____, K. Gao and D.B. Parsons, 1989: Numerical simulation of an intense squall line during 10-11 June 1985 PRE-STORM. Part I: Model verification. *Mon. Wea. Rev.*, **117**, 960-994.

_____ and J.M. Fritsch, 1986: Numerical simulation of the meso-β-scale structure and evolution of the 1977 Johnstown flood. Part I: Model description and verification. *J. Atmos. Sci.*, **43**, 1913-1943.

_____ and _____, 1988: A numerical investigation of a convectively generated inertially stable, extratropical warm-core mesovortex over land. Part I: Stricture and evolution. *Mon. Wea. Rev.*, **116**, 2660-2687.